JOC The Journal of Organic Chemistry

Article

pubs.acs.org/joc

# DDQ-Supported Alkoxylation of 2-Aza-21-carbaporphyrin and Noncatalyzed Transetherification of Its 3,21-Dialkoxy Derivatives

Xiaofang Li,*[,†] Bin Liu,[†] Xin Xu,[†] and Piotr J. Chmielewski*[,‡]

[†]Key Laboratory of Theoretical Chemistry and Molecular Simulation of Ministry of Education, Hunan Province College Key Laboratory of QSAR/QSPR, School of Chemistry and Chemical Engineering, Hunan University of Science and Technology, Xiangtan, Hunan 411201, China

[‡]Department of Chemistry, University of Wrocław, 14 F. Joliot-Curie Street, 50 383 Wrocław, Poland

Supporting Information

**ABSTRACT:** An oxidative addition of primary alkoxyls into two sites of N-confused porphyrin (NCP) has been accomplished by means of alcohols in the presence of a stoichiometric amount of 2,3-dichloro-5,6-dicyano-1,4-benzoquinone (DDQ). The resulting aromatic monocationic species **1**-$R_3$ (R = Me, Et) were characterized by the NMR and, in the case of triethoxy-NCP, by monocrystal X-ray diffraction analysis. One alkoxy group is located in position 3, on the macrocycle's perimeter, while two −OR moieties are attached to the internal carbon (position 21) of the *confused* pyrrole. The 3-EtO-21-Cl-NCP **2**, which is formed as a byproduct, was also structurally characterized by means of X-ray diffraction. Reduction of 3-RO-21-$(RO)_2$-NCP with hydrazine hydrate gave selectively a neutral and intrinsically chiral 3,21-bis(alkoxy)NCP **3**-$R_2$. Dealkylation of the externally bonded 3-OR fragment under basic conditions leading to a zwitterionic aromatic 3-oxo-species **4**-$R_2$, which still possesses the internal ketal functionality, was established by the NMR and X-ray diffraction methods. An unprecedented transetherification for the internal alkoxyl of **3**-$R_2$ can be achieved under very mild conditions and without catalyst. One of the alkoxyl-exchange products, i.e., 3-ethoxy-21-methoxy-NCP, was characterized by the X-ray diffraction method. The substitution proceeds via an associative ($S_N2$) mechanism resulting in an inversion of the chirality of **3**-RR′, which was shown by means of the NMR and chirooptical methods.

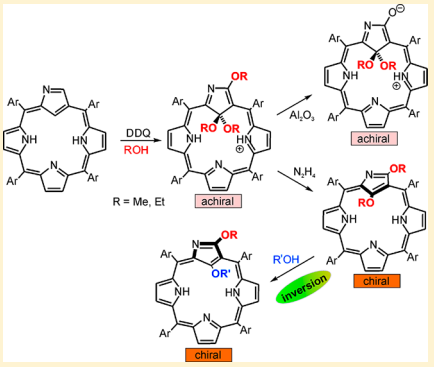


## INTRODUCTION

Porphyrins and their analogues and homologues are macrocyclic systems which are very broadly spread in pure and applied chemistry owing to their versatile redox, acid−base, optical, and coordination properties. The attractiveness of porphyrinoids is *inter alia* due to their reactivity which allows profound modification of the structure or properties of the system without destruction of the macrocyclic ring.

2-Aza-21-carbaporphyrin, also known as N-confused porphyrin (NCP),[1−5] an isomer of porphyrin of the same skeleton of macrocyclic ring, shares part of the reactivity with its regular congeners[6] offering some new features which are related to the presence of the *confused* pyrrole. The "unsubstituted" atoms of this moiety, i.e., external nitrogen (N2),[7−10] external carbon (C3),[11−18] and internal carbon (C21),[9,17−31] are particularly prone to various types of substitution, addition, oxidation, or ring fusion[8,13,16−18,32−37] reactions. Also very interesting and rich is the coordination chemistry of NCP and its derivatives. The presence of a donor site on the macrocycle's perimeter allows preparation of a variety of complexes in which both macrocyclic interior and peripheral atoms can be involved in bond formation with cations[8,9,26,38−43] or anions.[44−47]

In our search for facile modifications resulting in fine-tuned NCP systems that may serve as ligands in chiral organometallic complexes, we have applied several synthetic approaches such as reaction with dipolar agents[36,37] or active methylene reagents[14] allowing introduction of a substituent or substituents on the macrocycle's perimeter. In the present paper we report reactivity of the NCP ring that yields a system bearing alkoxy substituents on both external and internal carbon of the *confused* pyrrole. A 3-methoxylated derivative has been first obtained by Furuta et al. upon transformation of N-fused porphyrin under basic conditions.[16] More recently was reported the formation of externally alkoxylated systems which can be obtained from the silver(III) complexes of NCP.[48] The 21-RO-substituted derivatives of N-confused porphyrin have not been obtained to date, although an efficient method of $FeCl_3$-supported internal alkoxylation of benzocarbaporphyrin yielding carbaporphyrinoids with ketal functionality has been reported by Lash et al.[49] Inspired by this, we decided to apply an oxidative addition as a synthetic path of introduction of alkoxyls into NCP.

## RESULTS AND DISCUSSION

Unlike the case for benzocarbaporphyrins,[49,50] upon refluxing of NCP with ferric chloride in the presence of methanol, a dimeric iron(III) complex of 2-aza-21-oxocarbaporphyrin[51] is

**Received:** July 24, 2012
**Published:** August 27, 2012





dx.doi.org/10.1021/jo301573e | J. Org. Chem. 2012, 77, 8206−8219

formed rather than 21-bis(alkoxy)NCP, which we established on the basis of mass spectrometry indicating composition of the product and $^1$H NMR revealing its paramagnetic character. The mechanism of the oxidative addition reaction involves the formation of porphyrin radical species as an active intermediate,[50] thus the oxidation potential of the applied agent should be sufficiently high to oxidize NCP. On the other hand the oxidant ideally should act "tracelessly", without introduction of oxygen atom, metal ion, or other substituent into the porphyrin. Application of a strong organic oxidant, i.e., 2,3-dichloro-5,6-dicyano-1,4-benzoquinone (DDQ), in place of $FeCl_3$ allowed overcoming most of these problems. The syntheses were carried out in the presence of six equivalents of DDQ in the refluxing THF/ROH mixture (80/20 v/v, R = Me, Et) for 2 h (Scheme 1). The deep green adducts **1**-$R_3$ were

**Scheme 1. Alkoxylation of NCP**

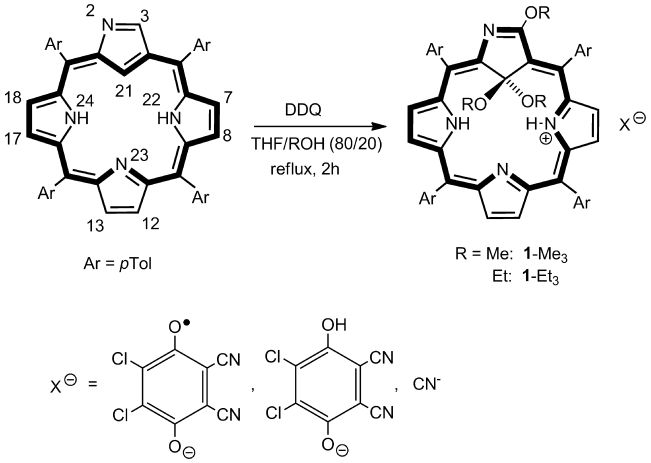


separated from the red and brownish products of the DDQ reduction by silica gel column chromatography and characterized by mass spectrometry, which revealed molecular ion peaks, indicating the presence of three alkoxy groups in each case.

Initially, we experienced some problems with the NMR characterization of these products because the $^1$H NMR spectra recorded for the $CDCl_3$ or $CD_2Cl_2$ solutions consisted of broad signals without fine structure of the spin−spin coupling (Figure 1A). We suspected that the observed line broadening was due to the presence of a radical species which was formed upon reduction of DDQ and interacted with **1**-$R_3$. In fact, electron paramagnetic resonance (EPR) spectra indicated the presence of a semiquinone-type anion radical $DDQ^{\bullet-}$ at $g$ = 2.0052 (Figure 1) which is a one-electron reduction product of the quinone.[52,53] The interaction between this paramagnetic species and the macrocycle is likely due to cationic character of the latter. In more polar solvents like methanol or acetonitrile the tight ion pair is effectively dissociated and the well-resolved $^{13}$C and $^1$H NMR spectra can be obtained (Figure 1B).

The $^1$H NMR spectra in $CD_3CN$ indicate aromaticity of **1**-$R_3$ and the presence of two protons located on the inner nitrogens of the porphyrinoid in line with the proposed structure of the monocation (Scheme 1). An indication for the monocationic character of these species comes from the mass of the molecular ion in the high-resolution ESI mass spectra showing no additional proton attached upon ionization to **1**-$R_3$ (see Supporting Information). The 22- and 24-NH resonate at about 4.2 and 4.4 ppm and were assigned on the basis of the COSY (coupling with $\beta$ protons of pyrrole) and NOESY (through-space contacts with protons of the substituent at C21) experiments as well as by the deuterium isotope exchange with $CD_3OD$. The chemical shift of the NH protons in **1**-$R_3$ is strongly affected by the intramolecular hydrogen bond that involves alkoxylic oxygens as the H-bond acceptors. Thus, the shielding effect of the aromatic ring which resulted in an upfield shift of the protons inside the macrocyclic crevice of unaltered porphyrins (about −2.8 ppm for NH's in regular tetraaryl porphyrins or NCP) is competing in **1**-$R_3$ with the downfield shift due to formation of the H-bonds. Integration of the signals in the $^1$H NMR spectra revealed the presence of two equivalent alkoxyls attached to the internal carbon and the one bound on the macrocycle's perimeter. The protons of the alkyls located inside the macrocycle are affected by the aromatic ring current, and their resonances are shifted upfield to the region from about −0.1 to nearly −1.8 ppm. The alkoxyl protons attached to the carbon directly bound to the oxygen correlate in the $^1$H,$^{13}$C HMBC spectrum with a carbon resonating near $\delta_C$ 96 ppm which is the $sp^3$-hybridized C21 strongly downfield shifted due to bonding of two oxygens. The methylene protons of the "internal" substituents in **1**-$Et_3$ are diastereotopically differentiated reflecting lack of "in-plane" symmetry of the macrocycle. On the other hand, methylene of the "external" ethoxyl is not diastereotopic indicating equivalence of both faces of the macrocyclic ring. In both adducts the external carbon C3 which resonates at about $\delta_C$ 177 ppm correlates in the HMBC spectrum with the protons of the "external" alkoxyl unequivocally indicating position of this substituent.

The cation−anion interaction of the macrocycle and $DDQ^{\bullet-}$ is apparently strong enough to make both components migrate together as a tight ion pair through the chromatographic column. The presence of an organic anion prevents crystallization of the system, but our efforts to exchange it into other counterions resulted in lack of reaction or further alteration of **1**-$R_3$ (vide infra). We expected that application of lower amounts of DDQ would force it to act as a two-electron oxidant and that the resulting reduction product would be solely a diamagnetic hydroquinone-type anion. Indeed, the reaction of NCP carried out under slightly modified conditions, i.e., with lower than stoichiometric amount of the DDQ oxidant (4−5 equiv), allowed separation of adducts which are diamagnetic and can be characterized by $^1$H and $^{13}$C NMR also in less polar solvents (e.g., $CDCl_3$, Figure 2A). Obviously, the yield is lower than upon application of the stoichiometric amount of DDQ (about 50%), but a benefit of this is crystallization ability of the obtained product.

The X-ray diffraction data analysis was performed for a single crystal of **1**-$Et_3$ confirming all the structural features of the systems in the solid that were derived from the NMR data in solution (Figure 3, Table S1 in Supporting Information). The presence of two ethoxyls attached to C21 and located on opposite sides of the porphyrin plane as well as one EtO group attached to C3 is apparent. The macrocyclic ring is flat, and a mean deviation from the plane defined by 24 heavy atoms of the porphyrin ($P_{24}$) is only 0.12 Å. The distances between internal C21 and neighboring C1 or C4 are 1.527(6) or 1.508(5) Å, respectively revealing single bonds. The sum of the bond angles around C21 is 657.2(3)°, which is the value expected for a pyramidal geometry of carbon environment (6 × 109.5° = 657°). Despite pyramidal environment of C21, the


dx.doi.org/10.1021/jo301573e | J. Org. Chem. 2012, 77, 8206−8219

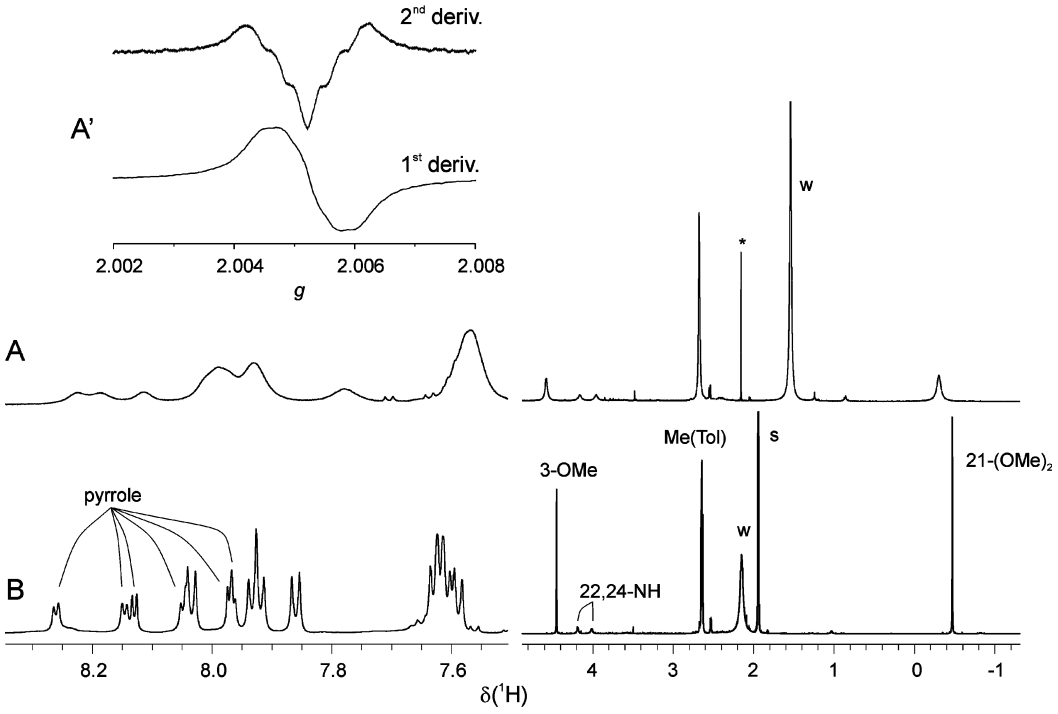


**Figure 1.** $^{1}$H NMR spectrum (600 MHz, 300 K) of **1**-$Me_3$ in $CDCl_3$ (A) and in $CD_3CN$ (B). The inset A′ comprises an EPR spectrum (1st and 2nd derivatives) of the **1**-$Me_3$ solution in chloroform recorded at room temperature. Note the presence of a five-component hyperfine structure which is clearly seen on the second derivative of the EPR signal and which is due to the unpaired electron coupling with two $^{14}$N nuclei of the $DDQ^{\bullet-}$. Signal of the dissolved water, residual proton solvent, and solvent impurity in the NMR spectra are denoted w, s, and *, respectively.

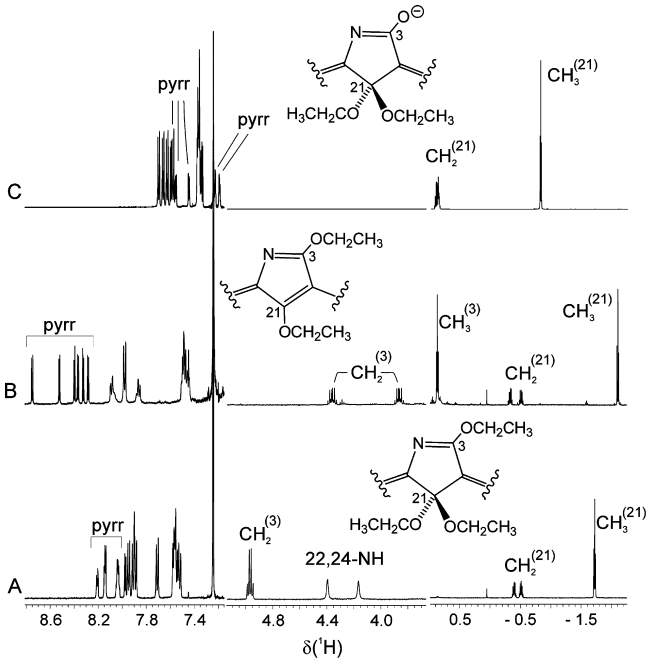


**Figure 2.** Comparison of the $^{1}$H NMR spectra (600 MHz, $CDCl_3$, 300 K) of **1**-$Et_3$ (A), **3**-$Et_2$ (B), and **4**-$Et_2$ (C). Labeling of the signals: pyrr, $\beta$-pyrrole protons; $CH_2^{(3)}$, $CH_3^{(3)}$, $CH_2^{(21)}$, $CH_3^{(21)}$ signals of methylene- and methyl-protons of the ethoxyls bound to carbon 3 or 21, respectively.

*confused* pyrrole is planar (mean deviation from the C1N2C3C4C21 plane is 0.014 Å) and it is almost coplanar with the rest of the macrocycle. A dihedral angle between its mean plane and $P_{21}$, that is, a mean plane defined by 21 heavy atoms of the ring, i.e., all except N2, C3, and C21, is only 7.1°. In fact, much more pronounced deviation from the coplanarity with the macrocycle is observed for the two "regular" pyrroles which are cis with respect to that *confused*. Thus, N22 lies 0.19 Å under the $P_{21}$, while N24 lies 0.33 Å over the plane. Such a deviation is clearly due to formation of the intramolecular H-bonds with the oxygens attached to C21 (Table S2 in Supporting Information). The hydrogen bond formation forces nitrogen and, consequently, the whole pyrrole unit to tip toward one of the oxygen atoms. Formation of the H-bonds involving internal protons is in line with the $^{1}$H NMR data given above. A cyanide counteranion can be identified in the crystal lattice disordered over two nonequivalently occupied positions. The source of this ion can be DDQ, for which a transfer of the cyano group onto the NCP has been reported.[54]

Under oxidant-deficient conditions (5 equiv of DDQ, 1.5 h of reflux) we also observed formation of a product which included a covalently bound substituent derived from the DDQ, namely, 3-ethoxy-21-chloro-NCP **2** (Chart 1). This olive-green derivative was formed with about 20% yield and accompanied the main product **1**-$Et_3$. The composition of **2** was derived from ESI HRMS ($m/z$ 749.3030, calcd 749.3042 for $[M + H]^+$), and its optical and NMR spectra revealed its aromaticity. The UV−vis spectrum of **2** is very similar to that of NCP[1] or its 21-alkylated derivatives[21,25,31] and clearly differs from that of **1**-$Et_3$ (Figure 4). The $^{1}$H NMR of **2** comprises neither 21-H nor ethoxyl signals in the high-field region. The only feature in this region is a very broad signal centered at about $\delta$ 0 ppm ($CDCl_3$, 300 K), which splits into two much narrower resonances located at −2.56 and −2.85 ppm when the spectrum is recorded at 213 K. These signals are attributed to 22- and 24-NH, i.e., internal protons of the 21-Cl-substituted macrocycle. The six $\beta$-pyrrole protons resonate in the region of $\delta$ 8.3−8.9 ppm characteristic for the aromatic NCP derivatives.


dx.doi.org/10.1021/jo301573e | J. Org. Chem. 2012, 77, 8206−8219

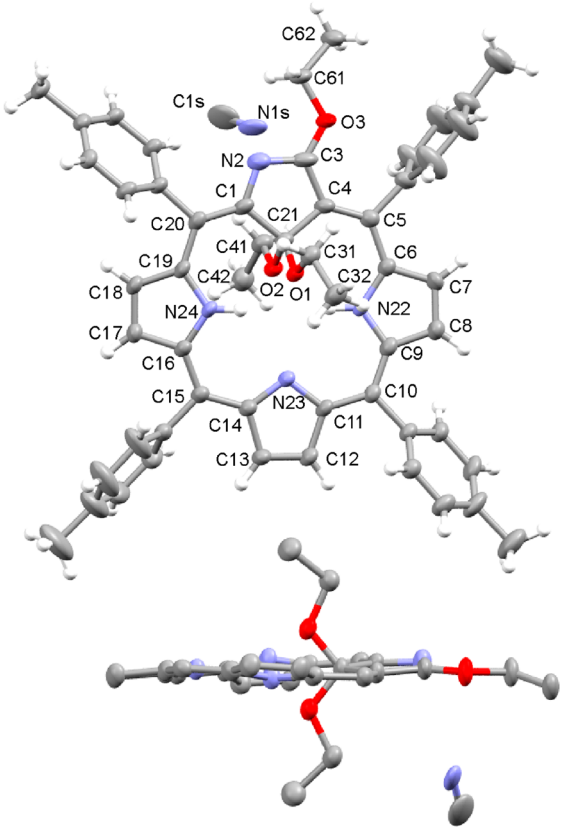


**Figure 3.** Perspective views and atom numbering of the molecular structure of **1**-$Et_3$ drawn with the 50% thermal displacement ellipsoids. Only the more occupied site of the anion is shown. In the lower view all hydrogen atoms and *meso*-tolyl substituents have been omitted for clarity.

**Chart 1**

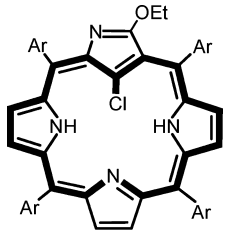


**2**

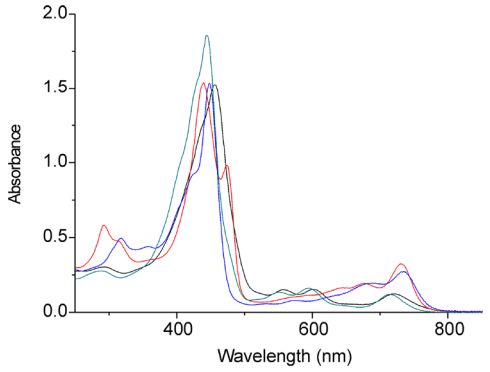


**Figure 4.** Optical spectra (dichloromethane, 298 K) of **1**-$Et_3$ (red), **2** (black), **3**-$Et_2$ (green), and **4**-$Et_2$ (blue).

There is a lack of signal of proton 3, and instead, there are three resonances of an ethyl group of the ethoxyl attached to this position: the triplet at $\delta$ 0.85 ppm represents methyl, while two multiplets (doublets of quartets) at $\delta$ 4.32 and 3.69 ppm ($CDCl_3$, 300 K) are signals of a diastereotopic methylene fragment. Both methylene protons correlate in the $^1H,^{13}C$ HMBC with a carbon resonating at $\delta_C$ 155.1 ppm which can be assigned to C3. Diastereotopic differentiation of the peripherally bound methylene protons clearly indicates nonplanarity of the porphyrin and, thus, its intrinsic chirality. Intriguingly, despite electronegative chlorine substituent bound to it, the internal carbon C21 resonates at $\delta_C$ 93.8 ppm, i.e., about 6 ppm upfield with respect to that in the unsubstituted NCP.[7] Such an upfield shift may indicate some inclination of C21 toward a pyramidal geometry.

The single crystal X-ray diffraction analysis of **2** confirmed both composition and the structure of this species (Figure 5,

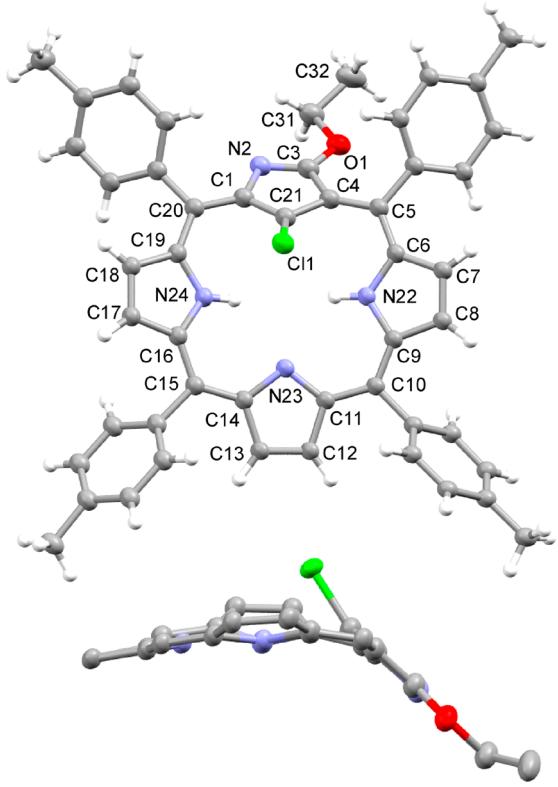


**Figure 5.** Perspective views and atom numbering of the molecular structure of **2** drawn with the 50% thermal displacement ellipsoids. In the lower view all hydrogen atoms and *meso*-tolyl substituents have been omitted for clarity. Arbitrarily, only enantiomer *R* is presented.

Table S1 in Supporting Information). The most striking structural feature of **2** is a very strong deviation of the *confused* pyrrole from the mean plane of the macrocycle. A dihedral angle between the mean plane of the *confused* pyrrole and that defined by the heavy atoms of the rest of the macrocycle ($P_{21}$) is 44.8°. Thus, chlorine is located 1.61 Å above $P_{21}$, while O1 2.15 Å, and the terminal ethyl carbon C32, 3.37 Å under this plane. The confused pyrrole is planar with a mean displacement of 0.004 Å. Also O1 attached to C3 lies in this plane with deviation of only 0.074 Å, while internally bound Cl1 resides 0.455 Å above the mean plane of the *confused* pyrrole indicating some pyramidal distortion of the trigonal C21. Also torsion angles C3C4C21Cl1 (−161.8(5)°) and N2C1C21Cl1


dx.doi.org/10.1021/jo301573e | J. Org. Chem. 2012, 77, 8206−8219

**Scheme 2. Reduction and Dealkylation of Tris(alkoxy)NCP and Transetherification of Bis(alkoxy)NCP**

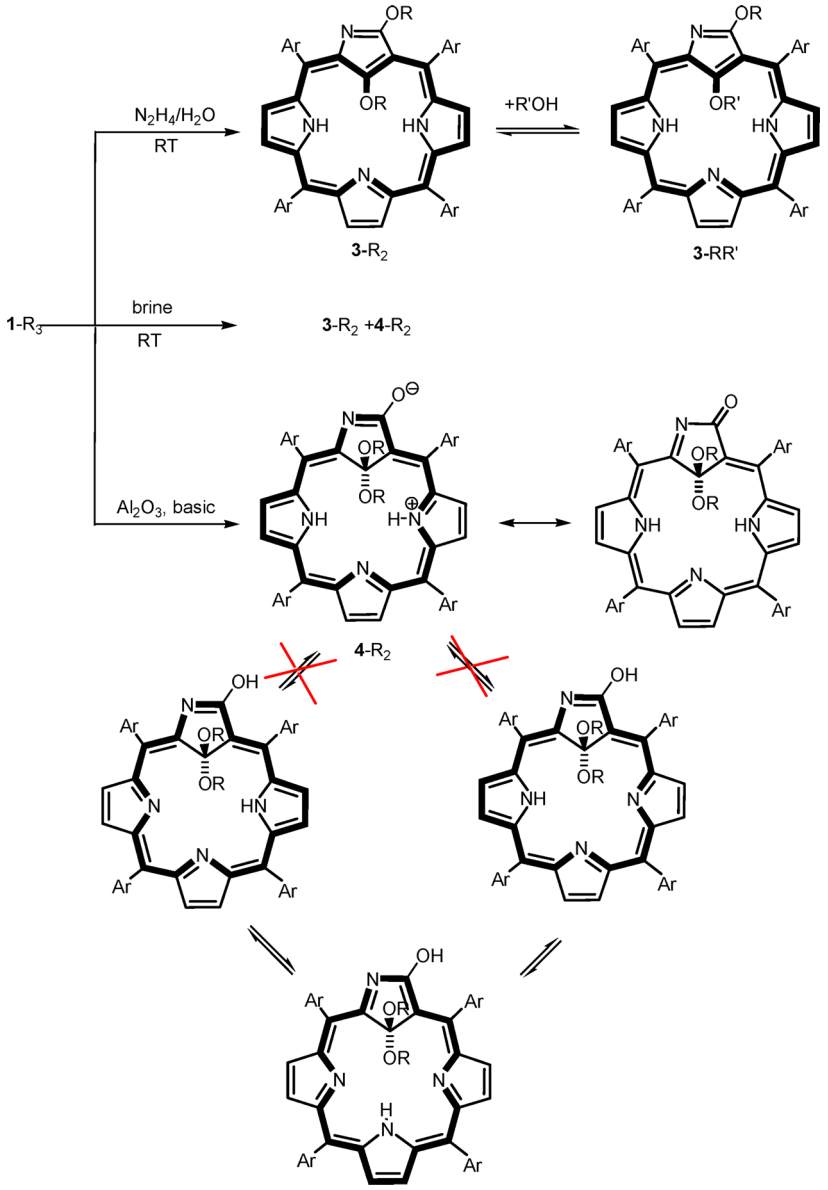


(161.8(5)) strongly deviate from the value of ±180° expected for the planar arrangement. For comparison, the torsion angles C1N2C3O1 and C21C4C3O1 are 176.7(6) and −176.0(6) in line with the in-plane situation of the oxygen attached to C3 and trigonal hybridization of this carbon. Unlike in **1**, the hydrogen-bearing pyrrole nitrogens are tipped to opposite direction than the substituent on C21 which makes H-bond formation with chlorine unlikely (Table S2 in Supporting Information). The molecule is chiral, but it crystallizes in a centrosymmetric space group, thus the crystal is a racemate and the unit cell contains a symmetry-related pair of enantiomers.

An analogous chlorine-substituted derivative has been previously obtained and structurally characterized by Lash for benzocarbaporphyrin.[50] The structural features revealed for chlorinated carbaporphyrin are similar to those of **2** except for chirality and substitution pattern on the macrocyclic perimeter. The case of **2** indicates that DDQ can also act as a source of chlorine, though it seems much less obvious than it is for $FeCl_3$.

Although ketal **1**-$R_3$ is formally a derivative of the cyclic ketone, i.e., 21-oxo-2-aza-21-carbaporphyrin, and liberation of this species upon application of a strong acid should be possible, our attempt to hydrolyze **1**-$R_3$ with trifluoroacetic acid or concentrated hydrochloric acid yielded, after neutralization, two new products but none of them with C═O functionality on C21. These products appeared also upon our other attempt aiming on the anion exchange with chloride by means of shaking of **1**-$R_3$ in dichloromethane solution with brine (Scheme 2). The mass spectrometry revealed that product **3**-$R_2$ contained two alkoxyls, while product **4**-$R_2$ comprised two alkoxyls and one oxo functionality.

The bis(alkoxy)NCP product **3**-$R_2$ can be readily obtained by reduction of **1**-$R_3$ with aqueous hydrazine hydrate. Right after mixing of the tris(alkoxy) derivative solution in dichloromethane with a drop of 40% solution of $N_2H_4$, the organic layer turned brown-red, and the olive-green color of it can be recovered by washing with several portions of water. The bis(alkoxy)NCP is practically the only product of the reaction, thus it can be obtained with a high yield. We performed the reduction for both alkoxy derivatives (Scheme 2) and characterized the products by high-resolution mass spectrom-


dx.doi.org/10.1021/jo301573e | J. Org. Chem. 2012, 77, 8206−8219

etry and UV−vis and NMR spectroscopies. Integration of the signals in $^1$H NMR spectra revealed that the porphyrinoids **3**-$R_2$ consisted of one alkoxyl bound to C3 and the other attached to C21, which means that reduction was combined with an abstraction of −OR group from the inner carbon. Protons of the alkoxyls located on C21 are shielded by the ring current of the porphyrin and resonate in a region of $\delta$ −0.5 to −2.0 ppm, while resonances of the externally bound substituent appear around $\delta$ 4.1 ppm (Figure 2B). The methylene protons of ethoxyls located both inside and outside the porphyrin crevice are diastereotopic, indicating chirality of the system due to its nonplanarity (Figure 2B). The aromaticity of **3**-$R_2$ is enhanced with respect to that of **1**-$R_3$, which is indicated by wider spreading of the proton signals with $\Delta\delta$ 11 ppm for bis(ethoxy)NCP as compared to $\Delta\delta$ 10 ppm for tris(ethoxy)-NCP (Figure 2). In fact, positions of $\beta$-pyrrole protons are similar to those in the $^1$H NMR spectrum of **2** or NCP. The signals of 22,24-NH are hardly seen at room temperature due to a fast chemical exchange causing their considerable broadening. At lower temperature, however, they appear as reasonably narrow singlets at $\delta$ −1.19 and −1.69 ppm (**3**-$Et_2$, $CDCl_3$, 223 K). Significantly, they are more than 1 ppm less shifted upfield than the signals of analogous protons in **2**, likely due to intramolecular H-bond formation with oxygen attached to C21 in **3**-$Et_2$. The signal of C21 in the $^{13}$C NMR spectrum of **3**-$R_2$ can be assigned on the basis of correlations with alkoxyl protons observed in the HMBC experiment. It appears at $\delta_C$ 131.3 ppm in the spectrum of **3**-$Et_2$ and at $\delta_C$ 133.1 ppm in that of **3**-$Me_2$, which is more than 30 ppm downfield with respect to the signal of the unsubstituted C21 of NCP.[7] Certainly, a major contribution to such deshielding influence has a binding of electronegative oxygen atom, but it is also likely that downfield shift is caused in part by less effective shielding of C21 by the ring current due to out-of plane position of this carbon with respect to the aromatic macrocycle. The signal of C3 can be found at $\delta_C$ 158.5 ppm, which is only 2 ppm more downfield than in the case of NCP[7] despite the presence of the oxygen-containing substituent at this carbon in **3**-$Et_2$. Optical spectra of **3**-$R_2$ resemble those of **2** or NCP (Figure 4).

The product **4**-$R_2$ can also be effectively obtained simply by passing solution of **1**-$R_3$ in dichloromethane through a basic alumina column of low activity (Brockman III). In fact, we intended to obtain **1**-$R_3$ in a neutral form by abstracting one of the internal NH's, but instead, a dealkylation of the external oxygen occurred, while both 22- and 24-NH remained inside the porphyrin core (Scheme 2). The optical spectrum of **4**-$R_2$ to some extent resembles that of **1**-$R_3$ in particular in the Q-band region (Figure 4), thus similar electronic structure for both derivatives could be anticipated. An integral intensity of the $^1$H NMR signal of the alkoxyl substituents indicates the presence of two −OR groups and their magnetic equivalence, while the upfield position of these resonances is in line with the location of them onto C21 as it took place in **1**-$R_3$ (Figure 2C). The aromatic ring current effect in **4**-$R_2$ is severely reduced with respect to that of **1**-$R_3$. Signals of the $\beta$-pyrrole protons appear in a narrow region of 7.2−7.6 ppm, and the most downfield shifted signal is due to one of the ortho-protons of the *meso*-tolyl substituent ($\delta$ 7.7 ppm, $CD_2Cl_2$, 300 K), while the most upfield shifted signal attributed to 21-methoxyl can be found at $\delta$ 0.79 ppm in the spectrum of **4**-$Me_2$ and in the case of **4**-$Et_2$ the triplet of terminal methyl is observed at $\delta$ −0.82 ppm (Figure 2C). Thus, the signals are spread over the region of only about 8.5 ppm. The aromaticity decrease can be interpreted as a contribution of a carbonyl-containing canonical form for which the delocalization path of the $\pi$-electrons is broken due to inclusion of one electron pair into C═O double bond, and which is consequently nonaromatic (Scheme 2). The observed ring current, though much weaker than in the case of cationic **1**-$R_3$, along with the presence of two protons inside the porphyrin crevice implies zwitterionic character of **4**-$R_2$ with a negative charge localized on the external oxygen. The weak aromaticity of this derivative is responsible for a poor shielding of the porphyrin interior, and thus, the 22,24-NH's resonate at $\delta$ 6.75 and 6.47 ppm. It is also likely that deshielding due to formation of H-bonds with oxygens at C21 contributes to the downfield shift of these signals. Both internal protons seem to be held firmly at their positions which can be inferred from the fine structure of the appropriate signals of $\beta$-pyrrole protons (7, 8, 17, and 18) due to spin−spin coupling with 22- and 24-NH which is observed even at room temperature. Thus, apparently the alternative tautomeric forms involving N2 or the oxygen bound to C3 as a proton sites do not occur at all in this system (Scheme 2).[55,56]

X-ray single crystal diffraction analysis performed for **4**-$Me_2$ reveals almost planar structure of the porphyrin ring, presence of two −OMe substituents attached to C21, and lack of an alkyl bound to O3 (Figure 6, Table S1 in Supporting Information). The C3−O3 distance is very short (1.175(5) Å) and definitely not compatible with a single bond formulation, for which a distance of about 1.30 Å is expected. Moreover, the N2−C3 distance (1.453(5) Å) is considerably longer than that in **1**-$Et_3$

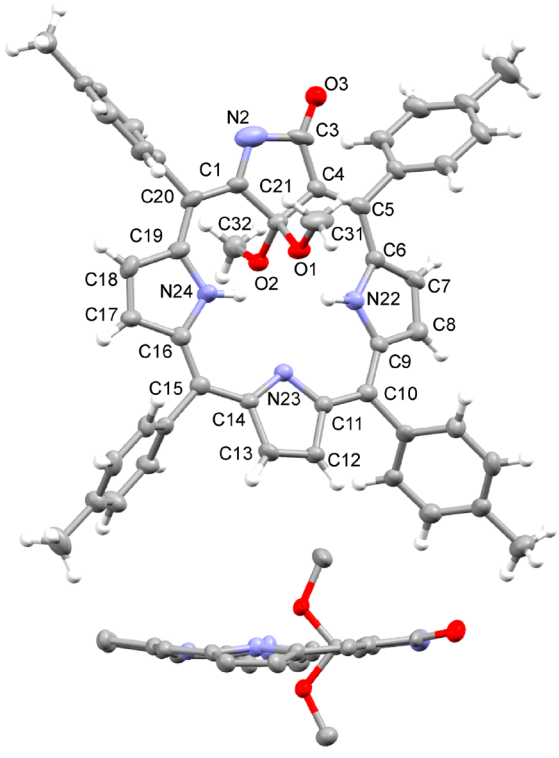


**Figure 6.** Perspective views and atom numbering of the molecular structure of **4**-$Me_2$ drawn with the 50% thermal displacement ellipsoids. Only the more populated form out of two present in the crystal lattice due to C3−N2 and O3 disorder is shown. Solvent (chloroform) molecules are omitted in both projections. In the lower view all hydrogen atoms and *meso*-tolyl substituents have been omitted for clarity.


dx.doi.org/10.1021/jo301573e | J. Org. Chem. 2012, 77, 8206−8219

(1.356(5) Å) or **2** (1.294(7) Å), which suggests weaker bond between these atoms in **4**-$Me_2$. Thus, the lactam functionality[12] can rather be assigned to this fragment of the *confused* pyrrole in the solid state. The structure of the macrocycle is otherwise close to that of **1**-$Et_3$. That includes the bond distances around C21 indicating $sp^3$ hybridization of this carbon (Table S1 in Supporting Information), planarity of the *confused* pyrrole, and its coplanarity with the rest of the porphyrin. Also the intramolecular H-bonds between internal nitrogens N22, N24 and O1, O2 are formed similarly effective to those observed in the structure of **1**-$Et_3$ (Table S2 in Supporting Information).

The structures of **2** and **3**-$R_2$ can also be subjected to further alteration. 21-Cl can be partially substituted with ethoxy group by 12 h reflux of **2** in the dichloromethane/EtOH (20:80) mixture resulting in about 50% conversion into **3**-$Et_2$. On the other hand, substitution of 21-OR in **3**-$R_2$ by other akoxyl is surprisingly facile. In some instances it can be accomplished at room temperature just by adding the incoming R′OH to the solution of **3**-$R_2$ (Scheme 2). For example, the complete exchange of the "internal" ethoxyl into methoxyl was observed about 8 h after addition of 70 equiv of MeOH to the solution of **3**-$Et_2$ in chloroform. The product **3**-EtMe can be transformed back to **3**-$Et_2$ by addition of an aliquot of ethanol (Figure 7).

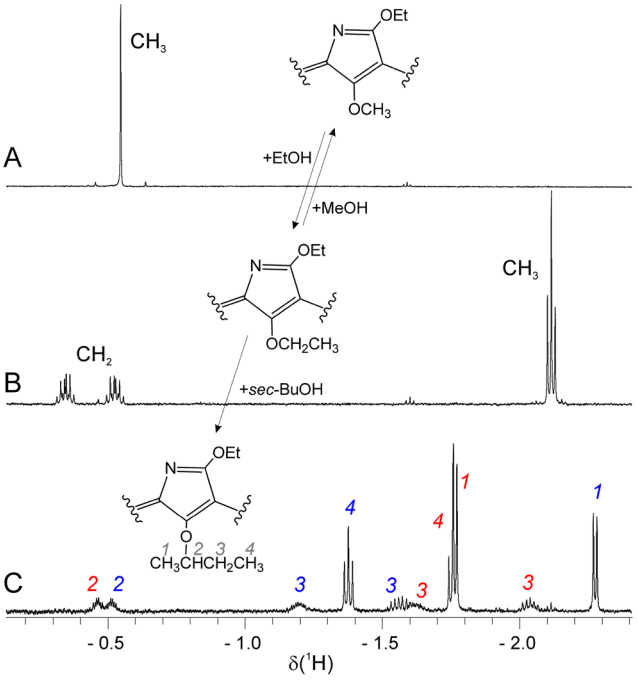


**Figure 7.** A high-field fragment of the $^1$H NMR spectra (600 MHz, $CDCl_3$, 300 K) of **3**-EtMe obtained from **3**-$Et_2$ by recrystallization from methanol (A), **3**-$Et_2$ obtained in situ from **3**-EtMe by addition of ethanol to the previous sample (B), and **3**-Et(*s*Bu) obtained from **3**-$Et_2$ by addition of 2-(*S*)-butanol (C). Note two sets of signals in C due to the presence of equally populated diastereomers.

The $^1$H NMR spectral characteristic of **3**-EtMe indicates unequivocally the presence of methoxyl substituent attached to C21 and ethoxyl group bound to C3. The rest of the spectrum is typical for the bis(alkoxy)NCP system **3**-$R_2$.

The single-crystal X-ray diffraction analysis of **3**-EtMe (Figure 8, Table S1 in Supporting Information) confirms the presence of different substituents inside and outside the porphyrin ring. It also indicates a nonplanar structure of the

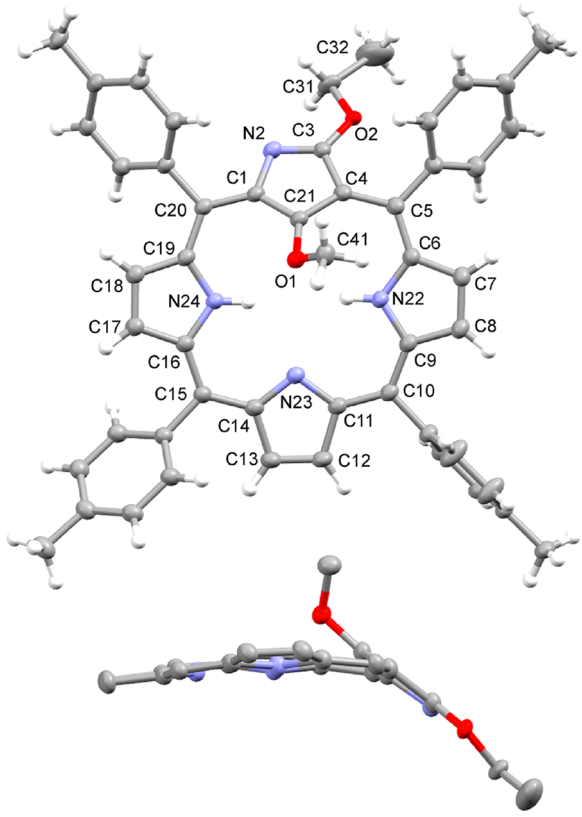


**Figure 8.** Perspective views and atom numbering of the molecular structure of **3**-EtMe drawn with the 50% thermal displacement ellipsoids. Arbitrarily, the enantiomer *R* has been chosen for presentations. In the lower view all hydrogen atoms and *meso*-tolyl substituents have been omitted for clarity.

porphyrin ring with the mean plane of the *confused* pyrrole tipped by 39.2° out of $P_{21}$ with N2 and C3 lying more than 1 Å over the $P_{21}$, and C21 about 0.3 Å under the plane. That causes chirality of the system, and the unit cell consists of a symmetry-related pair of enantiomers due to racemic character of the phase crystallizing in a centrosymmetric space group. The structure resembles that of **2** with one exception concerning much more in-plane situation of O1 with respect to the *confused* pyrrole in **3**-EtMe than it was in the case of C21-bound chlorine (vide supra). The displacement of O1 from the mean plane of the pyrrole is 0.049 Å while mean displacement of the atoms defining this plane is 0.034 Å. That is in line with a trigonal geometry of C21 in **3**-$R_2$ which seemed to be considerably pyramidally distorted in **2**. The distances between O1 and N22 or N24 as well as appropriate bond angles suggest interaction of the intramolecular H-bond-type in this system, though it seems to be weaker than in the case of **1**-$R_3$ or **4**-$R_2$ (Table S2 in Supporting Information).

Also some of the secondary alcohols can react with **3**-$R_2$ substituting internal alkoxyl, though the apparent reaction rate is significantly lower than in the case of the primary alcohols. For example, in the case of 2-butanol the full exchange of 21-EtO into 21-*s*BuO required altogether about 18 h of heating to 50 °C of the solution containing **3**-$Et_2$ in chloroform with 120 equiv of the secondary alcohol to achieve reaction completeness. Due to the intrinsic chirality of **3**-$R_2$ in the case of chiral alcohols such as 2-butanol or 1-phenylethanol a mixture of diastereomers is formed upon addition of pure enantiomer or racemic mixture of the alcohol. Thus, in the $^1$H NMR spectra


dx.doi.org/10.1021/jo301573e | J. Org. Chem. 2012, 77, 8206−8219

two sets of signals can be observed which are particularly strongly differentiated in the high-field part of the spectrum where resonances of the internal substituent can be found. Owing to that, the signal assignment to a particular stereoisomer in this region is feasible (Figure 7C) allowing also an assessment of the component molar ratios.

Chirality of **3**-$R_2$ is defined by an orientation of the atoms of *confused* pyrrole with respect to the direction of its deviation from the porphyrin plane (Figure 9). The configuration of such

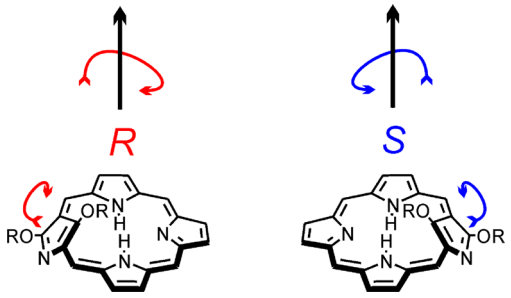


**Figure 9.** Definition of absolute configuration of **3**-$R_2$.

systems is stable as long as a substituent on C21 prevents flipping of the *confused* pyrrole, thus an attempt to separate the enantiomers was considered to be feasible. However, a chiral-phase HPLC of **3**-$Me_2$ resulted in a poor resolution despite several mobile and stationary phases tested. Nevertheless, an early fraction collected with dichloromethane/ethyl acetate as a mobile phase is optically active containing some excess of one of the enantiomers. Its CD spectrum consisted of several features, but the most pronounced Cotton effect appears at the wavelength of the Soret-type band, i.e., at about 445 nm (Figure 10). The spectrum pattern is very close to that observed previously for one of the enantiomers of 21-methylated NCP[31] for which absolute configuration has been established on the basis of TDDFT calculation and NMR and further confirmed by X-ray method applied for the dimeric derivatives.[57] Considering these structural and spectral similarities and according to the definition given in Figure 9,

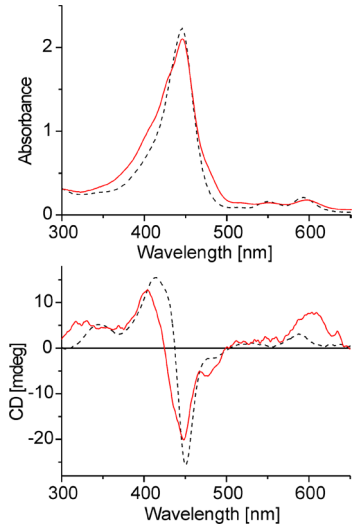


**Figure 10.** Comparison of the UV−vis (upper traces) and CD (lower traces) spectra of the enantiomer *R* of **3**-$Me_2$ (solid red line) and 21-methylated derivative of NCP (black dashed line).[31]

a configuration *R* can be assigned to the enantiomer of **3**-$Me_2$ displaying negative sign of the Cotton effect at a lower-energy part of the major CD signal. (Note the opposite configuration definition used in ref 31 due to a lack of the substituent at C3.)

A much more effective separation of the stereoisomers can be achieved for the derivative with a chiral substituent attached to C21, namely, for **3**-Me(*s*Bu). With an enantiomerically pure (*S*)-*sec*-butanol the substitution at C21 yields a mixture of diastereomers which differ only in configuration of the porphyrin ring, so their quantitative relations and optical activity are strictly related to the planar chirality of the macrocycle. In Figure 11 partial $^1$H NMR and CD spectra of

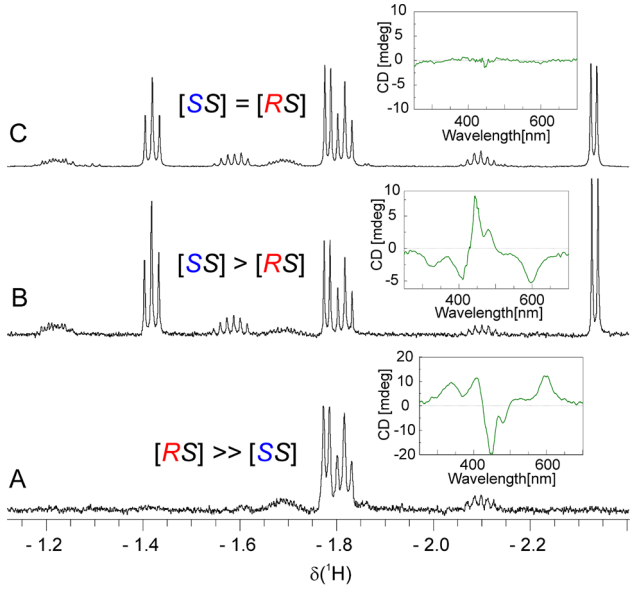


**Figure 11.** High-field fragments of the $^1$H NMR spectra ($CDCl_3$, 300 K) of diastereomer *RS* of **3**-Me(*s*Bu) (A), mixture containing 39% de of diastereomer *SS* (B), and the solution before separation consisting of an equimolar mixture of both diastereomers (C). In the insets associated with NMR traces the CD spectra recorded for each of the solutions are presented.

the major fractions obtained upon a chiral-phase HPLC of **3**-Me(*s*Bu) are presented. The diastereomer *RS* contained in the fastest migrating band can be obtained in a practically pure form, while the other stereoisomer, *SS*, can be separated only partially (diastereomer excess 39% or diastereomer ratio 1:0.44). Their configuration can be assigned on the basis of the CD spectra which are of the same pattern as the spectrum of nonracemic **3**-$Me_2$. The solution before the stereoisomer separation is optically inactive in the visible region (Figure 11C) because absorption of the chiral 2-butoxyl occurs in the far UV and does not interfere with that of the porphyrin ring.

Chirality of the system allows exploring some details of the mechanism of the transetherification in **3**-$R_2$. Usually the exchange of an −OR group requires an acidic catalyst and proceeds via a dissociative mechanism ($S_N1$) involving a relatively stable carbocation,[58−62] and in some instances an alkoxide anion facilitates ether bond cleavage.[63−65] Apparently, upon transetherification of **3**-$R_2$ no external catalyst is involved, thus the reagents need to activate each other in some way by a specific interaction involving structural fragments in the vicinity of the reaction site, i.e., C21. Such an interaction may also suggest an associative mechanism of the alkoxyl exchange.


dx.doi.org/10.1021/jo301573e | J. Org. Chem. 2012, 77, 8206−8219

A $^1$H NMR-monitored titration of **3**-Me$_2$ with 1-(*S*)-phenylethanol ($CDCl_3$, 300 K) resulted in a splitting of certain peaks into two components, and the difference of their chemical shifts grew as the concentration of alcohol increased with apparently no changes of their relative intensities. This behavior indicates formation of a supramolecular adduct between the alcohol and the porphyrin. Since both reagents are chiral, and **3**-Me$_2$ solution is racemic, the differentiation is due to the presence of *RS* and *SS* diastereomers of adduct which are expected to be NMR-distinguishable. No such effect is observed with *sec*-butanol as a titrant. We suppose that the source of the differentiation is the phenyl ring of phenylethanol and its distinct orientation in each diastereomer with respect to these *β*-pyrrole protons that are close to the alcohol binding site. Significantly, the strongest effect is observed for the proton in position 18, which is in the closest vicinity of the external nitrogen N2; the effect is much weaker for 17-H located on the same pyrrole unit, but does not occur for the other *β*-pyrrole protons, for which only a small downfield shift takes place over the alcohol concentration range of 0−120 equiv (Figure 12). It may suggest N2 as the alcohol binding site.

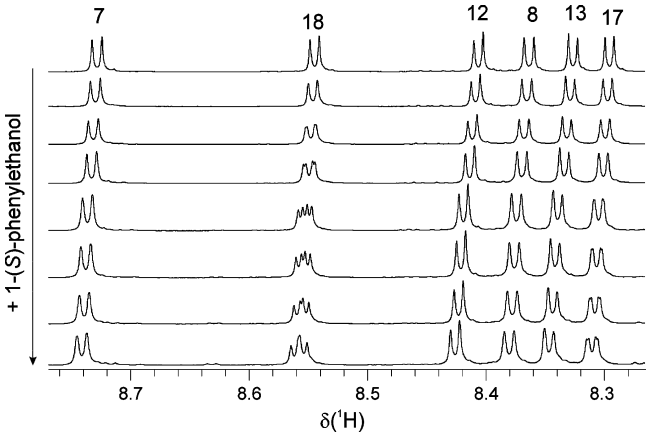


**Figure 12.** $^1$H NMR spectral changes in the low-field region of the spectra of **3**-Me$_2$ ($CDCl_3$, 300 K) recorded upon titration with 1-(*S*)-phenylethanol (0−120 equiv from the top to the bottom). The assignment of signals given on the top was made on the basis of low-temperature COSY and NOESY experiments.

Spectral changes due to substitution of 21-OMe with phenylethanol can be observed by $^1$H NMR almost immediately after addition of the incoming alcohol, though reaction is complete after several days. The reaction is stereoselective, although the selectivity is rather poor and, surprisingly, opposite on the early and final stages. In the beginning (after 1 h of the reaction) the diastereomer *RS* has higher concentration, while in the final reaction mixture stereoisomer *SS* dominates (de 8%, Figure 13). That domination allowed assignment of the NMR signals to the certain isomers on the basis of the CD spectra of the diastereomer mixtures. The diastereomeric excess in the early stages of the reaction reflects an affinity of the alcohol enantiomer toward one of the enantiomers of **3**-Me$_2$ and is likely kinetic in its origin as no steric preference in porphyrin−alcohol adduct formation has been observed (vide supra). However, domination of one of the diastereomers when reaction is completed implies change of the porphyrin configuration in a part of the reacting molecules. Otherwise, reaction for racemic mixture of **3**-Me$_2$ would result in a 1:1

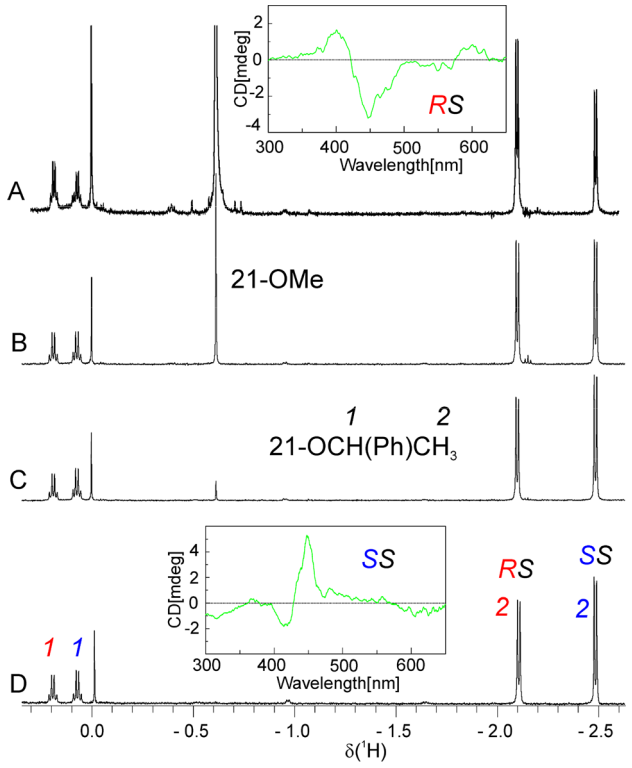


**Figure 13.** The high-field parts of the $^1$H NMR spectra ($CDCl_3$, 300 K) recorded after 1 h (A), 24 h (B), 48 h (C), and 6 days (D) after mixing **3**-Me$_2$ with 120 equiv of 1-(*S*)-phenylethanol. The spectral intensities were normalized with respect to the signals of the *SS* isomer. The insets present CD spectra of the initial and final solutions.

mixture of diastereomers of **3**-Me(PhEt). Since the configuration inversion is precluded in **3**-R$_2$ by the presence of the substituent at C21 which cannot be threaded through the porphyrin crevice, observation of an excess of one of the diastereomers suggests that one of the following processes occurred. (1) Dissociation of the C21−O1 bond which liberates the *confused* pyrrole to move C21 onto the opposite side before an attack of the incoming alkoxyl. Such a process, however, should result in a stochastic 1:1 mixture rather than induction of the diastereomeric excess as the attack from each of the sides of the porphyrin plane is equally probable.[25] (2) Formation of the ketal-type intermediate with different −OR groups on the opposite sides of the planar porphyrin ring and subsequent dissociation of the outgoing alkoxyls. In this case an inversion rather than racemization can be expected as long as a consecutive substitution is slow enough and an effective racemization is kinetically prevented.

To check which one of these mechanisms is operative in the present case we performed a series of exchange experiments for the optically active **3**-RR′ systems. Initially, we attempted substitution of the chiral *sec*-butoxyl of the pure diastereomer *RS* of **3**-Me(*s*Bu) in the reaction with methanol. However, the reaction proceeded very slowly even at 60 °C, and we were unable to achieve the full exchange of the alkoxyls, which prevented analysis of the optical activity of the formed compound. Moreover, the much faster consecutive reaction of the formed **3**-Me$_2$ with excess of methanol causes effective racemization. The convincing results were derived from an experiment carried out for the solution containing an excess of the *R* enantiomer of **3**-Me$_2$ reacting with 2-(*S*)-butanol. The progress of the reaction was monitored by $^1$H NMR. After


dx.doi.org/10.1021/jo301573e | J. Org. Chem. 2012, 77, 8206−8219

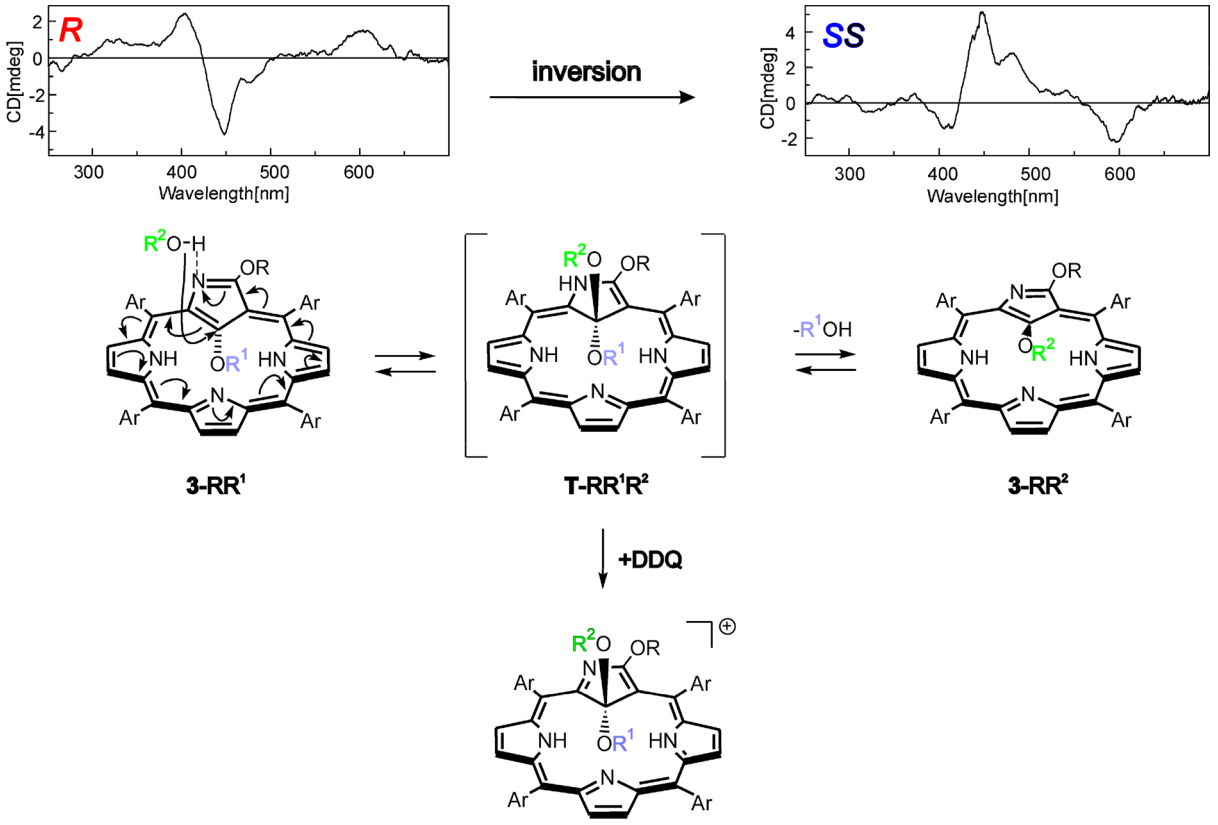


**Figure 14.** Top row: CD spectrum of the solution chloroform containing an excess of the *R* enantiomer of **3**-$Me_2$ (left) and of the same solution after 24 h of heating at 60 °C with 80 equiv of 2-(*S*)-butanol (right). Lower row: the mechanism of the transetherification of **3**-$R_2$ and the final step of formation of **1**-$RR^1R^2$.

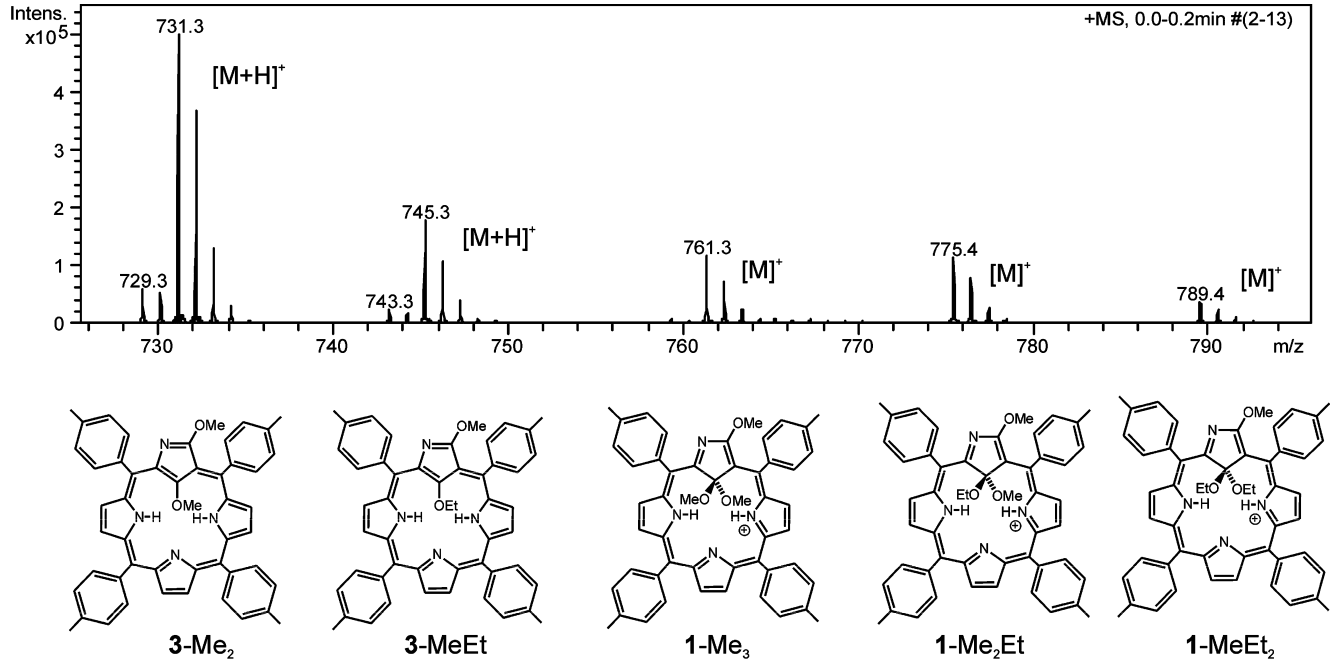


**Figure 15.** Mass spectrum (ESI-TOF) of the mixture formed upon addition of DDQ to the **3**-$Me_2$ + EtOH system.

about 24 h of heating of the solution to 50 °C, NMR indicated an excess of the *SS* diastereomer (de about 19%). The CD spectrum of this solution displays Cotton effects of opposite signs to those observed for the starting *R*-**3**-$Me_2$ (Figure 14). Clearly, the transetherification causes inversion of the porphyrin configuration, and that implies formation of an intermediate **T** whose structure consists of a planar ring and two alkoxyls attached simultaneously to C21 (Figure 14). Thus, the reaction mechanism is associative and the process can be described as $S_N2$.


dx.doi.org/10.1021/jo301573e | *J. Org. Chem.* 2012, 77, 8206–8219

It is also likely that a similar transient species is formed during synthesis of **1**-$R_3$ and the two-electron oxidation of **T**-$R_3$ by DDQ (formally a hydride abstraction) yields cationic ketal product. In fact, identification of **2** in the reaction mixtures indicates position 3 as a primary target of alkoxylation. Reaction may go further through 21-monoalkoxylated NCP with the final quenching of the equilibrium between **3**-$RR^2$ and **T** by oxidation. To check if such a synthetic path indeed occurs we add 1 equiv of DDQ to the solution of **3**-$Me_2$ in THF/EtOH mixture (80/20) at room temperature. The solution color changed immediately from olive-green to grass-green, which is typical for **1**-$R_3$. The products were analyzed by $^1$H NMR and ESI-MS (Figure 15), which indicate, among others (i.e., **1**-$Me_3$, **1**-$MeEt_2$, **3**-MeEt), the presence of the cationic product **1**-$Me_2Et$ comprising both methoxyl and ethoxyl substituent bound to C21 confirming occurrence of the intermediate **T** both in substitution process **3**-$R_2$ and in the formation reaction of the triply alkoxylated NCP **1**-$R_3$.

## CONCLUSION

Introduction of three primary alkoxy groups to the *confused* pyrrole of NCP appears to be an efficient and easy to conduct modification of this porphyrinoid. Reactivity of the ketals **1**-$R_3$ allows further alteration of the macrocycle's structure and substitution pattern. The noncatalytic transetherification of **3**-$R_2$ occurring under very mild conditions is of special interest. The process is reversible and can be described as an example of dynamic covalent chemistry (DCC).[60,66−68] This reactivity can be exploited in the construction of more complex structures involving NCP derivatives such as oligomers or various types of complexes. The studies on these subjects are underway in our laboratories.

## EXPERIMENTAL SECTION

**General Methods.** Applied dichloromethane was freshly distilled from calcium hydride. Optical and circular dichroism spectra were recorded in dichloromethane. NMR spectra were recorded in $CD_3CN$, $CDCl_3$, or $CD_2Cl_2$ and referenced with residual solvent signals (1.94, 7.24, or 5.31, respectively). 2D experiments were performed by means of standard software. The low-temperature NOESY spectra were recorded with 2048 × 512 data blocks and with 400 ms mixing time. Resolution of stereoisomers was performed at room temperature by means of a Chirex 3010 analytical column (25 cm length, 4.6 mm i.d.) packed with 5 $\mu$m silica gel coated with covalently bound (*S*)-valine and dinitroaniline. The HPLC-grade solvents were applied. EPR spectra were recorded at room temperature for chloroform or acetonitrile solutions contained in capillary test tubes using X-band microwave radiation (9.752 GHz) with modulation frequency and amplitude 100 kHz and 0.2 G, respectively.

**Synthesis of Precursor.** Starting porphyrin NCP was synthesized as previously described.[3]

**Alkoxylation of NCP.** In a typical synthesis of **1**-$R_3$ a solution containing 100 mg of NCP (0.15 mmol) and 203 mg of 2,3-dichloro-5,6-dicyano-1,4-benzoquinone (0.9 mmol) dissolved in a mixture of THF/ROH (50 mL, 80/20 v/v, R = Me, Et) was refluxed for 2 h. Solvents were then removed, and solid residuum was dissolved in dichloromethane and passed down a silica gel column. The initial red and brown bands migrating with dichloromethane were discarded, and a grass-green fraction eluted with 20% of ethyl acetate in dichloromethane was collected. The solution volume was reduced, and the product was precipitated by addition of hexane as dark green powder. Yields: **1**-$Me_3$, 73 mg (68%); **1**-$Et_3$, 85 mg (71%).

*Selected data for* ***1****-*$Me_3$*:* mp >300 °C; $^1$H NMR (600 MHz, $CD_3CN$, 300 K) $\delta_H$ = 8.26 (d, $^3J$ = 4.7 Hz, 1H), 8.15 (d, $^3J$ = 4.7 Hz, 1H), 8.13 (d, $^3J$ = 4.5 Hz, 1H), 8.05 (d, $^3J$ = 4.7 Hz, 1H), 8.03 (d, $^3J$ = 7,8 Hz, 2H), 7.97 (d, $^3J$ = 4.5 Hz, 1H), 7.96 (d, $^3J$ = 4.5 Hz, 1H), 7.93 (d, $^3J$ = 7.7 Hz, 2H), 7.90 (d, $^3J$ = 7.7 Hz, 2H), 7.86 (d, $^3J$ = 7.8 Hz, 2H), 7.63 (d, $^3J$ = 7.8 Hz, 2H), 7.62 (d, $^3J$ = 7.7 Hz, 2H), 7.61 (d, $^3J$ = 7.8 Hz, 2H), 7.59 (d, $^3J$ = 7.7 Hz, 2H), 4.45 (s, 3H), 4.18 (b, 1H), 4.01 (b, 1H), 2.65 (s, 3H), 2.64 (s, 6H), 2.63 (s, 3H), −0.47 (s, 6H). $^1$H NMR (600 MHz, $CDCl_3$, 300 K) $\delta_H$ = 8.23 (dd, $^3J$ = 4.7 Hz, $^4J$ = 1.1 Hz, 1H), 8.17 (dd, $^3J$ = 4.7 Hz, $^4J$ = 1.4 Hz, 1H), 8.11 (d, $^3J$ = 4.5 Hz, 1H), 8.02 (dd, $^3J$ = 4.6 Hz, $^4J$ = 1.2 Hz, 1H), 7.97 (dd, $^3J$ = 4.7 Hz, $^4J$ = 1.1 Hz, 1H), 7.96 (d, $^3J$ = 4.5 Hz, 1H), 7.95 (d, $^3J$ = 7.8 Hz, 2H), 7.91 (d, $^3J$ = 7.8 Hz, 2H), 7.90 (d, $^3J$ = 7.8 Hz, 2H), 7.75 (d, $^3J$ = 7.6 Hz, 2H), 7.56 (d, $^3J$ = 7.6 Hz, 2H), 7.55 (d, $^3J$ = 7.8 Hz, 2H), 7.54 (d, $^3J$ = 7.6 Hz, 2H), 7.51 (d, $^3J$ = 7.7 Hz, 2H), 4.52 (s, 3H), 4.16 (b, 1H), 3.97 (b, 1H), 2.64 (s, 9H), 2.61 (s, 3H), −0.40 (s, 6H); $^{13}$C NMR (150 MHz, $CDCl_3$, 300 K) $\delta_C$ = 175.3, 174.5, 172.7, 171.3, 171.1, 161.8, 157.2, 155.4, 152.5, 146.0, 141.8, 141.6, 140.2, 140.2, 139.7, 138.9, 138.8, 138.2, 137.9, 136.8, 136.8, 136.5, 136.1, 135.0, 135.0, 134.9, 134.4, 133.8, 133.8, 133.7, 131.8, 129.7, 129.2, 129.0, 128.4, 128.4, 128.3, 118.6, 117.2, 113.1, 96.7, 89.0, 59.1, 49.0, 21.6, 21.5, 21.5; UV−vis ($CH_2Cl_2$, 298 K) $\lambda$/nm ($\varepsilon$/$M^{-1}$ $cm^{-1}$) = 256 (sh), 288 (26900), 318 (sh), 363 (sh) 441 (80500), 477 (50700), 571 (sh), 594(sh), 644 (sh), 678 (19300), 734 (17400); HRMS (ESI-TOF) $m/z$ = 761.3479 (obsd), 761.3486 (calcd for $C_{51}H_{45}N_4O_3$, $[M]^+$).

*Selected data for* ***1****-*$Et_3$*:* mp >300 °C; $^1$H NMR (600 MHz, $CD_3CN$, 300 K) $\delta_H$ = 8.23 (dd, $^3J$ = 5.0 Hz, $^4J$ = 1.81 Hz, 1H), 8.14 (d, $^3J$ = 4.7 Hz, 1H), 8.10 (dd, $^3J$ = 4.9 Hz, $^4J$ = 2.0 Hz, 1H), 8.05 (dd, $^3J$ = 4.7 Hz, $^4J$ = 2.0 Hz, 1H), 8.01 (d, $^3J$ = 8.1 Hz, 2H), 8.00 (dd, $^3J$ = 4.6 Hz, $^4J$ = 2.3 Hz, 1H), 7.97 (d, $^3J$ = 4.7 Hz, 1H), 7.93 (d, $^3J$ = 7.8 Hz, 2H), 7.91 (d, $^3J$ = 7.8 Hz, 2H), 7.83 (d, $^3J$ = 7.8 Hz, 2H), 7.616 (d, $^3J$ = 7.8 Hz, 2H), 7.614 (d, $^3J$ = 7.8 Hz, 2H), 7.611 (d, $^3J$ = 7.8 Hz, 2H), 7.57(d, $^3J$ = 7.9 Hz, 2H), 4.92 (q, $^3J$ = 7.2 Hz, 2H), 4.46 (b, 1H), 4.26 (b, 1H), 2.64 (s, 9H), 2.62 (s, 3H), 1.35 (t, $^3J$ = 7.2 Hz, 3H), −0.36 (dq, $^2J$ = 9.0 Hz, $^3J$ = 7.0 Hz, 2H), −0.47 (dq, $^2J$ = 9.0 Hz, $^3J$ = 7.0 Hz, 2H), −1.79 (t, $^3J$ = 7.0 Hz, 6H); $^{13}$C NMR (150 MHz, $CDCl_3$, 300 K) $\delta_C$ = 174.0, 172.8, 161.6, 157.0, 156.9, 152.9, 141.7, 141.1, 140.2, 140.1, 140.0, 139.6, 138.8, 138.7, 137.9, 137.8, 136.7, 136.5, 136.2, 135.1, 134.9, 134.7, 134.2, 133.8, 133.7, 131.5, 129.6, 129.2, 128.9, 128.5, 128.3, 118.1, 114.6 94.7, 68.4, 57.4, 31.6, 22.6, 21.5; UV−vis ($CH_2Cl_2$, 298 K) $\lambda$/nm ($\varepsilon$/$M^{-1}$ $cm^{-1}$) = 258 (sh), 288 (27900), 317 (sh), 356 (sh) 440 (81100), 477 (51600), 576 (sh), 594(sh), 643 (sh), 678 (11600), 734 (18200); HRMS (ESI-TOF) $m/z$ = 803.3953 (obsd), 803.3956 (calcd for $C_{54}H_{51}N_4O_3$, $[M]^+$).

**Separation of 3-Ethoxy-21-chloro-*meso*-(*p*-tolyl)-2-aza-21-carbaporphyrin 2.** 60 mg of NCP (0.09 mmol) and 100 mg of 2,3-dichloro-5,6-dicyano-1,4-benzoquinone (0.44 mmol) dissolved in a mixture of THF/EtOH (50 mL, 80/20 v/v) was refluxed for 1.5 h. Solvents were then removed, and solid residuum was dissolved in dichloromethane and passed down a silica gel column. The initial red and brown bands migrating with dichloromethane were discarded, and an olive-green fraction eluted with 5% of ethyl acetate in dichloromethane containing **2** was collected. The solution volume was reduced, and the product was precipitated as a dark green powder by addition of hexane. Yield: 18 mg (27%).

*Selected data for* ***2****:* mp 240−245 °C; $^1$H NMR (600 MHz, $CDCl_3$, 300 K) $\delta_H$ = 8.82 (d, $^3J$ = 4.9 Hz, 1H), 8.62 (d, $^3J$ = 4.7 Hz, 1H), 8.45 (d, $^3J$ = 4.7 Hz, 1H), 8.43 (d, $^3J$ = 4.9 Hz, 1H), 8.41 (d, $^3J$ = 4.7 Hz, 1H), 8.30 (d, $^3J$ = 8.0 Hz, 2H), 8.30 (d, $^3J$ = 4.7 Hz, 1H), 8.20 (d, $^3J$ = 7.7 Hz, 3H), 8.03 (d, $^3J$ = 7.6 Hz, 1H),7.94 (d, $^3J$ = 7.3 Hz, 1H),7.88 (d, $^3J$ = 7.7 Hz, 1H), 7.58 (d, $^3J$ = 8.6 Hz, 3H), 7.57 (d, $^3J$ = 7.9 Hz, 3H), 7.51 (d, $^3J$ = 7.7 Hz, 2H), 7.48 (d, $^3J$ = 7.7 Hz, 2H), 4.32 (dq, $^2J$ = 10.2 Hz, $^4J$ = 7.2 Hz, 1H), 3.69 (dq, $^2J$ = 10.2 Hz, $^4J$ = 7.2 Hz, 1H), 2.66 (s, 3H), 2.65 (s, 3H), 2.64 (s, 3H), 2.62 (s, 3H), 0.85 (t, $^3J$ = 7.0 Hz, 3H); $^{13}$C NMR (150 MHz, $CDCl_3$, 300 K) $\delta_C$ = 158.3, 155.4, 155.1, 144.8, 140.6, 139.0, 138.4, 138.2, 138.1, 137.6, 137.4, 137.2, 137.0, 136.9, 136.7, 135.9, 135.0, 134.9, 134.6, 134.4, 133.7, 128.4, 128.37, 128.0, 127.7, 127.6, 127.5, 126.8, 125.3, 125.1, 124.1,121.4, 121.3, 116.5, 93.8, 63.4, 21.55, 21.49, 21.45,13.9; UV−vis ($CH_2Cl_2$, 298 K) $\lambda$/nm ($\varepsilon$/$M^{-1}$ $cm^{-1}$) = 295 (21500), 350 (sh), 438 (sh), 458 (108000), 559 (10700), 602 (10900), 723 (8700); HRMS (ESI-TOF) $m/z$ = 749.3030 (obsd), 749.3042 (calcd for $C_{50}H_{42}ClN_4O$, $[M + H]^+$).


dx.doi.org/10.1021/jo301573e | *J. Org. Chem.* 2012, 77, 8206−8219

**Reduction of Tris(alkoxy)-NCP.** In a typical procedure a sample of **1**-$R_3$ (30 mg, 0.04 mmol) dissolved in dichloromethane (5 mL) was shaken with aqueous hydrazine hydrate (0.5 mL, 40% solution) for 2 min, whereupon the organic phase turned brown-red. The reaction mixture was then washed with six portions of water (10 mL) until the organic phase turned olive-green. After chromatographic workup (silica gel column with dichlomethane/ethyl acetate as a mobile phase) the product **3**-$R_2$ was precipitated with hexane as an olive powder. Yields: **3**-$Me_2$, 25 mg (85%); **3**-$Et_2$, 27 mg (84%).

*Selected data for **3**-$Me_2$:* mp >260 °C; $^1$H NMR (600 MHz, $CDCl_3$, 300 K) $\delta_H$ = 8.73 (d, $^3J$ = 4.9 Hz, 1H), 8.54 (d, $^3J$ = 4.6 Hz, 1H), 8.40 (d, $^3J$ = 4.6 Hz, 1H), 8.36 (d, $^3J$ = 5.0 Hz, 1H), 8.32 (d, $^3J$ = 4.6 Hz, 1H), 8.29(d, $^3J$ = 4.6 Hz, 1H), 8.10 (b, 1H),8.08 (dd, $^3J$ = 7.8 Hz, $^4J$ = 1.8 Hz, 1H), 8.03 (d, $^3J$ = 7.8 Hz, 2H),7.98 (d, $^3J$ = 7.6 Hz, 1H), 7.88 (dd, $^3J$ = 7.7 Hz, $^4J$ = 1.8 Hz, 1H),7.50 (d, $^3J$ = 7.9 Hz, 4H),7.47 (d, $^3J$ = 7.9 Hz, 1H),7.46 (d, $^3J$ = 7.9 Hz, 1H), 7.45 (d, $^3J$ = 7.9 Hz, 1H), 3.66 (s, 3H), 2.64 (s, 3H), 2.63 (s, 3H), 2.62 (s, 3H), 2.60 (s, 3H), −0.54 (s, 3H); $^{13}$C NMR (126 MHz, $CDCl_3$, 300 K) $\delta_C$ = 158.3, 158.2, 154.7, 140.4, 139.5, 139.2, 138.4, 137.5, 137.3, 137.1, 137.04, 136.98, 136.93, 136.8, 136.7, 136.2, 135.7, 134.8, 134.3, 134.23, 134.17, 134.1, 133.4, 132.7, 128.2, 128.1, 127.8, 127.52, 127.50, 127.4, 126.66, 125.61, 125.3, 123.5, 121.3, 119.8, 115.3, 115.2, 56.5, 54.8, 21.48, 21.472, 21.469, 21.45; UV−vis ($CH_2Cl_2$, 298 K) $\lambda$/nm ($\varepsilon$/$M^{-1}$ $cm^{-1}$) = 270 (20100), 407 (sh), 430 (sh), 446 (105700), 518 (sh), 548 (7300), 597 (8900), 651 (sh), 716 (7500); HRMS (ESI-TOF) $m/z$ = 731.3365 (obsd), 731.3381 (calcd for $C_{50}H_{43}N_4O_2$, $[M + H]^+$).

*Selected data for **3**-$Et_2$:* mp >260 °C; $^1$H NMR (600 MHz, $CDCl_3$, 300 K) $\delta_H$ = 8.75 (d, $^3J$ = 5.0 Hz, 1H), 8.52 (d, $^3J$ = 4.7 Hz, 1H), 8.40 (d, $^3J$ = 4.7 Hz, 1H), 8.37 (d, $^3J$ = 4.9 Hz, 1H), 8.32 (d, $^3J$ = 4.6 Hz, 1H), 8.28 (d, $^3J$ = 4.7 Hz, 1H), 8.09 (dd, $^3J$ = 7.6 Hz, $^4J$ = 1.8 Hz, 1H), 8.07 (b, 1H), 7.98 (d, $^3J$ = 7.9 Hz, 2H), 7.88 (b, 1H), 7.8 (dd, $^3J$ = 7.6 Hz, $^4J$ = 1.8 Hz, 1H), 7.50−7.45 (overlapping multiplets, 8H), 4.36 (dq, $^2J$ = 10.5 Hz, $^3J$ = 7.1 Hz, 1H), 3.86 (dq, $^2J$ = 10.5 Hz, $^3J$ = 7.1 Hz, 1H), 2.64 (s, 3H), 2.63 (s, 3H), 2.61 (s, 3H), 2.59 (s, 3H), 0.86 (t, $^3J$ = 7.1 Hz, 1H), −0.34 (dq, $^2J$ = 9.9 Hz, $^3J$ = 6.9 Hz, 1H), −0.51 (dq, $^2J$ = 9.9 Hz, $^3J$ = 6.9 Hz, 1H), −2.10 (t, $^3J$ = 6.9 Hz, 1H); $^{13}$C NMR (126 MHz, $CDCl_3$, 300 K) $\delta_C$ = 158.5, 157.9, 154.6, 140.0, 139.6, 139.3, 138.8, 137.9, 137.6, 137.1, 137.1, 136.9, 136.8, 136.74, 136.67, 136.2, 135.6, 134.7, 134.6, 134.3, 134.2, 134.1, 134.0, 133.3, 131.4, 128.04, 127.97, 127.7, 127.5, 127.43, 127.41, 126.5, 1253, 125.2, 123.4, 121.2, 120.0, 116.7, 115.3, 65.1, 62.8, 21.49, 21.47, 21.4, 13.8, 10.7; UV−vis ($CH_2Cl_2$, 298 K) $\lambda$/nm ($\varepsilon$/$M^{-1}$ $cm^{-1}$) = 270 (20100), 402 (sh), 428 (sh), 448 (101900), 517 (sh), 551 (8100), 598 (9100), 648 (sh), 715 (7800); HRMS (ESI-TOF) $m/z$ = 759.3682 (obsd), 759.3694 (calcd for $C_{52}H_{47}N_4O_2$, $[M + H]^+$).

**Exchange of the Alkoxyl Substituent at C21 (Transetherification).** In a typical procedure, to the solution of **3**-$R_2$ (5 mg) in chloroform (0.7 mL) was added an excess of alcohol (20−200 equiv). The reaction progress was monitored by $^1$H NMR. For primary alcohols the reaction was complete after 12 h. In the cases of secondary alcohols (2-butanol, 1-phenylethanol) the solution was heated to 50 °C for three days. The solvents were then removed, and solid residue was dissolved in a minimum amount of dichloromethane and precipitated by addition of hexane as an olive powder. Yields: quantitative.

*Selected data for **3**-EtMe:* mp 205−210 °C; $^1$H NMR (600 MHz, $CDCl_3$, 300 K) $\delta_H$ = 8.76 (d, $^3J$ = 5.0 Hz, 1H), 8.54 (d, $^3J$ = 4.6 Hz, 1H), 8.41 (d, $^3J$ = 4.6 Hz, 1H), 8.38 (d, $^3J$ = 5.0 Hz, 1H), 8.33 (d, $^3J$ = 4.6 Hz, 1H), 8.29 (d, $^3J$ = 4.6 Hz, 1H), 8.09 (dd, $^3J$ = 7.5 Hz, $^4J$ = 2.2 Hz, 1H), 8.01 (d, $^3J$ = 8.1 Hz, 2H),7.99 (b, 1H), 7.88 (dd, $^3J$ = 7.2 Hz, $^4J$ = 2.0 Hz, 1H), 7.87 (d, $^3J$ = 8.0 Hz, 1H), 7.50 (d, $^3J$ = 8.1 Hz, 1H),7.49 (d, $^3J$ = 8.1 Hz, 2H), 7.49 (d, $^3J$ = 7.9 Hz, 2H), 7.47 (d, $^3J$ = 7.2 Hz, 1H), 7.45 (d, $^3J$ = 8.1 Hz, 1H), 7.44 (d, $^3J$ = 8.0 Hz, 1H), 4.34 (dq, $^2J$ = 10.4 Hz, $^3J$ = 7.0 Hz, 1H), 3.84 (dq, $^2J$ = 10.4 Hz, $^3J$ = 7.0 Hz, 1H), 2.64 (s, 3H), 2.63, (s, 3H), 2.61 (s, 3H), 2.60, (s, 3H), 0.86 (t, $^3J$ = 7.0 Hz, 3H), −0.55 (s, 3H); $^{13}$C NMR (150 MHz, $CDCl_3$, 300 K) $\delta_C$ = 158.1, 158.0, 154.7, 140.3, 139.6, 139.2, 138.7, 137.6, 137.2, 137.1, 137.0, 136.92, 136.87, 136.8, 136.2, 135.7, 134.8, 134.7, 134.3, 134.2, 134.1, 134.0, 133.3, 129.1, 129.1, 128.7, 128.6, 128.1, 127.9, 127.7, 127.52, 127.48, 127.44, 126.6, 125.3, 125.2, 123.5, 121.3, 120.0, 115.9, 115.3, 62.9, 56.6, 21.5, 21.4, 13.8; MS (ESI-TOF) $m/z$ = 745.3522 (obsd), 745.3537 (calcd for $C_{51}H_{45}N_4O_2$, $[M + H]^+$)

*Selected data for **3**-Et(sBu):* $^1$H NMR (600 MHz, $CDCl_3$, 300 K) $\delta_H$ = 8.74 (d, $^3J$ = 4.7 Hz, 1H), 8.50 (d, $^3J$ = 4.7 Hz, 1H), 8.37 (d, $^3J$ = 4.7 Hz, 1H), 8.35 (d, $^3J$ = 4.7 Hz, 1H), 8.29 (d, $^3J$ = 4.6 Hz, 1H), 8.25 (d, $^3J$ = 4.7 Hz, 1H), 8.11 (dd, $^3J$ = 7.9 Hz, $^4J$ = 1.9 Hz, 1H), 8.08 (b, 1H),7.97 (d, $^3J$ = 7.9 Hz, 2H),7.86 (d, $^3J$ = 7.5 Hz, 1H), 7.79 (d, $^3J$ = 7.9 Hz, 1H), 7.49 (d, $^3J$ = 7.9 Hz, 2H), 7.48 (d, $^3J$ = 7.9 Hz, 2H), 4.35 (dq, $^2J$ = 10.4 Hz, $^3J$ = 7.2 Hz, 1H), 3.84 (dq, $^2J$ = 10.4 Hz, $^3J$ = 7.1 Hz, 1H), 2.64 (s, 3H), 2.63 (s, 3H), 2.61 (s, 3H), 2.59 (s, 3H), 0.85 (t, $^3J$ = 7.3 Hz, 3H), −0.45 (m, 1H), −1.60 (m, 1H), −1.75 (t, $^3J$ = 7.6 Hz, 3H), −1.76 (d, $^3J$ = 6.5 Hz, 3H), −2.02 (m, 1H) diastereomer *RS*; 8.73 (d, $^3J$ = 4.9 Hz, 1H), 8.50 (d, $^3J$ = 4.6 Hz, 1H),8.37 (d, $^3J$ = 4.6 Hz, 1H), 8.35 (d, $^3J$ = 4.9 Hz, 1H), 8.30 (d, $^3J$ = 4.6 Hz, 1H), 8.26 (d, $^3J$ = 4.6 Hz, 1H), 8.09 (dd, $^3J$ = 7.9 Hz, $^4J$ = 2.0 Hz, 1H), 7.97 (d, $^3J$ = 7.9 Hz, 2H), 7.94 (d, $^3J$ = 7.9 Hz, 1H), 7.89 (d, $^3J$ = 7.9 Hz, 1H),7.83 (dd, $^3J$ = 7.9 Hz, $^4J$ = 1.8 Hz, 1H), 7.50 (d, $^3J$ = 8.0 Hz, 2H), 7.48 (d, $^3J$ = 7.9 Hz, 2H), 4.35 (dq, $^2J$ = 10.6 Hz, $^3J$ = 7.2 Hz, 1H), 3.85 (dq, $^2J$ = 10.6 Hz, $^3J$ = 7.7 Hz, 1H), 2.64 (s, 3H), 2.63 (s, 3H), 2.61 (s, 3H),2.59 (s, 3H), 0.85 (t, $^3J$ = 7.6 Hz, 3H), −0.50 (m, 1H), −1.19 (m, 1H), −1.36 (t, $^3J$ = 6.7 Hz, 3H), −1.55 (m, 1H), −2.27 (t, $^3J$ = 6.7 Hz, 3H) diastereomer *SS*; $^{13}$C NMR (150 MHz, $CDCl_3$, 300 K) $\delta_C$ = 158.1, 157.98, 157.94, 154.6, 140.1, 139.7, 139.4, 138.9, 137.7, 137.1, 137.0, 136.8, 136.75, 136.69, 134.8, 134.5, 134.2, 134.12, 134.06, 133.2, 130.8, 128.8, 128.0, 127.8, 127.7, 127.46, 127.40, 127.3, 126.4, 125.0, 123.4, 123.3, 121.1, 117.5, 117.4, 115.2, 76.3, 68.2, 26.8, 24.0, 23.8, 23.2, 23.0, 22.7, 21.5, 21.3, 14.1, 13.8, 11.0, 6.0; HRMS (ESI-TOF) $m/z$ = 787.4001 (obsd), 787.4007 (calcd for $C_{54}H_{51}N_4O_2$, $[M + H]^+$).

*Selected data for **3**-Me(sBu):* $^1$H NMR (600 MHz, $CDCl_3$, 300 K) $\delta_H$ = 8.71 (d, $^3J$ = 4.9 Hz, 1H), 8.51 (d, $^3J$ = 4.6 Hz, 1H), 8.37 (d, $^3J$ = 4.6 Hz, 1H), 8.34 (d, $^3J$ = 4.6 Hz, 1H), 8.29 (d, $^3J$ = 4.9 Hz, 1H), 8.25 (d, $^3J$ = 4.6 Hz, 1H), 8.10 (dd, $^3J$ = 7.5 Hz, $^4J$ = 2.2 Hz, 1H), 8.00 (d, $^3J$ = 8.0 Hz, 2H), 7.93 (d, $^3J$ = 7.9 Hz, 1H), 7.88 (d, $^3J$ = 7.9 Hz, 1H), 7.80 (dd, $^3J$ = 7.5 Hz, $^4J$ = 2.2 Hz, 1H), 7.50 (d, $^3J$ = 8.0 Hz, 4H), 7.49 (d, $^3J$ = 7.9 Hz, 4H), 3.67 (s, 3H), 2.64 (s, 3H), 2.63 (s, 3H), 2.62 (s, 3H), 2.60 (s, 3H), −0.45 (m, 1H), −1.63 (m, 1H), −1.73 (d, $^3J$ = 6.1 Hz, 3H), −1.76 (t, $^3J$ = 7.5 Hz, 3H), −2.05 (m, 1H) diastereomer *RS*; 8.70 (d, $^3J$ = 4.9 Hz, 1H), 8.51 (d, $^3J$ = 4.6 Hz, 1H), 8.37 (d, $^3J$ = 4.6 Hz, 1H), 8.34 (d, $^3J$ = 4.9 Hz, 1H), 8.29 (d, $^3J$ = 4.6 Hz, 1H), 8.26 (d, $^3J$ = 4.6 Hz, 1H), 8.08 (dd, $^3J$ = 7.5 Hz, $^4J$ = 1.9 Hz, 1H), 8.00 (d, $^3J$ = 7.9 Hz, 2H), 7.92 (d, $^3J$ = 7.9 Hz, 1H), 7.90 (d, $^3J$ = 8.0 Hz, 1H), 7.84 (dd, $^3J$ = 7.7 Hz, $^4J$ = 1.9 Hz, 1H), 7.50 (d, $^3J$ = 7.9 Hz, 2H), 7.49 (d, $^3J$ = 8.0 Hz, 2H), 7.45 (d, $^3J$ = 7.6 Hz, 2H), 3.67 (s, 3H), 2.64 (s, 3H), 2.63 (s, 3H), 2.61 (s, 3H), 2.60 (s, 3H), −0.51 (m, 1H), −1.17 (m, 1H), −1.36 (t, $^3J$ = 7.4 Hz, 3H), −1.53 (m, 1H), −2.29 (d, $^3J$ = 6.1 Hz, 3H) diastereomer *SS*; $^{13}$C NMR (150 MHz, $CDCl_3$, 300 K) $\delta_C$ = 175.0, 158.4, 158.3, 158.1, 158.0, 154.7, 140.20, 140.19, 139.70, 139.69, 139.34, 139.33, 138.6, 137.67, 137.65, 137.26, 137.25, 137.23, 137.22, 137.06, 137.05, 136.95, 136.94, 136.85, 136.81, 136.79, 136.2, 136.1, 135.7, 135.6, 134.8, 134.6, 134.22, 134.16, 134.13, 134.11, 134.10, 134.06, 133.3, 128.2, 127.9, 127.8, 127.5, 127.43, 127.37, 126.5, 125.6, 125.5, 125.2, 125.13, 123.43, 123.37, 121.17, 121.15, 119.97, 119.91, 116.8, 116.7, 115.3, 76.29, 76.26, 54.8, 26.7, 24.0, 23.8, 21.48, 21.47, 21.46, 21.45, 14.1, 13.9, 5.9, 5.4; HRMS (ESI-TOF) $m/z$ = 773.3848 (obsd), 773.3850 (calcd for $C_{53}H_{49}N_4O_2$, $[M + H]^+$).

*Selected data for **3**-Me(PhEt):* $^1$H NMR (600 MHz, $CDCl_3$, 300 K) $\delta_H$ = 8.80 (d, $^3J$ = 4.9 Hz, 1H),8.54 (d, $^3J$ = 4.7 Hz, 1H),8.41 (d, $^3J$ = 4.9 Hz, 1H),8.37 (d, $^3J$ = 4.6 Hz, 1H), 8.32 (d, $^3J$ = 4.6 Hz, 1H),8.30 (d, $^3J$ = 4.9 Hz, 1H),8.15 (d, $^3J$ = 7.5 Hz, 1H),8.01 (d, $^3J$ = 7.8 Hz, 2H), 7.95 (d, $^3J$ = 7.3 Hz, 2H),7.83 (d, $^3J$ = 7.3 Hz, 2H), 7.52−7.44 overlapping doublets of both diastereomers, 6.83 (t, $^3J$ = 7.2 Hz, 1H), 6.58 (t, $^3J$ = 7.2 Hz, 2H), 4.66 (d, $^3J$ = 7.2 Hz, 2H), 3.57 (s, 3H), 2.65 (s, 3H), 2.65 (s, 3H), 2.62 (s, 3H), 2.58 2.62 (s, 3H), 0.13 (q, $^3J$ = 6.6 Hz, 1H), −2.43 (t, $^3J$ = 6.6 Hz, 3H) major ($x$ = 0.54) diastereomer *SS*; 8.70 (d, $^3J$ = 5.0 Hz, 1H), 8.61 (d, $^3J$ = 4.4 Hz, 1H), 8.35 (d, $^3J$ = 4.6 Hz, 1H), 8.32 (d, $^3J$ = 5.0 Hz, 1H), 8.29 (d, $^3J$ = 4.4 Hz, 1H), 8.25 (d, $^3J$ = 4.6 Hz, 1H),8.09 (d, $^3J$ = 8.0 Hz, 2H),7.91 (d, $^3J$ = 7.6 Hz, 1H), 7.87 (d, $^3J$ = 7.6 Hz, 1H), 7.73 (d, $^3J$ = 8.0 Hz, 2H), 7.52−7.44 overlapping doublets of both diastereomers, 6.67 (t, $^3J$ = 7.2 Hz, 1H),


dx.doi.org/10.1021/jo301573e | J. Org. Chem. 2012, 77, 8206−8219

6.33 (t, $^3J$ = 7.3 Hz, 2H), 4.34 (d, $^3J$ = 7.3 Hz, 2H), 3.60 (s, 3H), 2.65 (s, 3H), 2.64 (s, 3H), 2.62 (s, 3H), 2.59 (s, 3H), 0.25 (q, $^3J$ = 6.6 Hz, 1H), −2.04 (t, $^3J$ = 6.6 Hz, 3H) minor ($x$ = 0.46) diastereomer *RS*; $^{13}$C NMR (150 MHz, $CDCl_3$, 300 K) $\delta_C$ = 158.7, 158.0, 154.7, 140.0, 139.75, 139.67, 139.4, 139.3, 138.5, 137.8, 137.51, 137.46, 137.1, 137.0, 136.9, 136.8, 136.7, 136.4, 136.3, 135.9, 135.0, 134.9, 134.6, 134.5, 134.2, 134.15, 134.10, 133.3, 133.2, 128.5, 128.4, 128.3, 128.0, 127.9, 127.8, 127.6, 127.5, 127.4, 127.3, 127.0, 126.6, 126.4, 125.4, 125.2, 125.1, 124.9, 124.7, 123.5, 123.3, 121.2, 120.9, 119.8, 115.3, 78.1, 54.73, 54.68, 25.1, 21.5, 17.8, 14.1; HRMS (ESI-TOF) $m/z$ = 821.3832 (obsd), 821.3850 (calcd for $C_{57}H_{49}N_4O_2$, $[M + H]^+$).

**Dealkylation of Tris(alkoxy)-NCP.** In a typical procedure a sample of **1**-$R_3$ (15 mg, 0.02 mmol) was dissolved in dichloromethane. The solution was then put on the top of the chromatographic column filled with basic aluminum oxide (Brockman III). The column was then charged with dichloromethane, and the first band containing a small amount (less than 10%) of **3**-$R_2$ was collected. The mobile phase was than changed to a 1% mixture of ROH and dichloromethane, and a grass-green solution was eluted. The solvents were evaporated. The black-green crystals of the product **4**-$R_2$ were obtained by slow diffusion of hexane into dichloromethane solution. Yields: **4**-$Me_2$, 13 mg (87%); **4**-$Et_2$, 12 mg (77%).

*Selected data for* ***4****-$Me_2$:* mp >300 °C; $^1$H NMR (600 MHz, $CDCl_3$, 300 K) $\delta_H$ = 7.69 (d, $^3J$ = 7.9 Hz, 2H), 7.65 (d, $^3J$ = 7.8 Hz, 2H), 7.64 (d, $^3J$ = 7.9 Hz, 2H), 7.62 (d, $^3J$ = 4.6 Hz, 1H), 7.61 (d, $^3J$ = 7.8 Hz, 2H), 7.60 (d, $^3J$ = 5.2 Hz, 1H), 7.51 (dd, $^3J$ = 5.2 Hz, $^4J$ = 1.6 Hz, 1H), 7.43 (d, $^3J$ = 7.9 Hz, 2H), 7.42 (d, $^3J$ = 7.8 Hz, 2H), 7.41 (d, $^3J$ = 7.8 Hz, 2H), 7.40 (d, $^3J$ = 7.6 Hz, 2H), 7.36 (d, $^3J$ = 4.6 Hz, 1H), 7.28 (dd, $^3J$ = 4.5 Hz, $^4J$ = 2.5 Hz, 1H), 7.25 (dd, $^3J$ = 4.5 Hz, $^4J$ = 2.1 Hz, 1H), 6.75 (b, 1H), 6.46 (b, 1H), 2.57 (s, 3H), 2.55 (s, 3H), 2.54 (s, 3H), 2.53 (s, 3H), 0.79 (s, 6H); $^{13}$C NMR (150 MHz, $CDCl_3$, 300 K) $\delta_C$ = 181.1, 172.2, 165.0, 154.9, 151.6, 143.0, 139.1, 138.8, 138.7, 138.5, 138.1, 138.1, 137.9, 137.6, 137.4, 137.1, 136.4, 136.0, 135.3, 133.9, 133.6, 133.5, 132.1, 131.9, 131.7, 131.6, 129.0, 128.8, 128.45, 128.38, 125.0, 123.7, 122.3, 115.7, 108.8, 100.0, 50.4, 21.8, 21.70, 21.66; UV−vis ($CH_2Cl_2$, 298 K) $\lambda$/nm ($\varepsilon$/$M^{-1}$ $cm^{-1}$) = 320 (33800), 359 (30100), 408 (sh), 426 (sh) 450 (107000), 523 (3600), 576 (5400), 627 (sh), 690 (13300), 737 (18600); HRMS (ESI-TOF) $m/z$ = 747.3337 (obsd), 747.3330 (calcd for $C_{50}H_{43}N_4O_3$, $[M + H]^+$).

*Selected data for* ***4****-$Et_2$:* mp >300 °C; $^1$H NMR (600 MHz, $CDCl_3$, 300 K) $\delta_H$ = 7.69 (d, $^3J$ = 7.9 Hz, 2H), 7.66 (d, $^3J$ = 8.0 Hz, 2H), 7.62 (d, $^3J$ = 7.9 Hz, 2H), 7.59 (d, $^3J$ = 4.6 Hz, 1H), 7.57 (d, $^3J$ = 8.0 Hz, 2H),7.55 (dd, $^3J$ = 5.2 Hz, $^4J$ = 2.1 Hz, 1H), 7.44 (dd, $^3J$ = 5.2 Hz, $^4J$ = 1.8 Hz, 1H), 7.37 (d, $^3J$ = 7.9 Hz, 2H), 7.36 (d, $^3J$ = 7.9 Hz, 4H),7.35 (d, $^3J$ = 8.0 Hz, 2H),7.33 (d, $^3J$ = 4.6 Hz, 1H), 7.23 (dd, $^3J$ = 4.3 Hz, $^4J$ = 2.5 Hz, 1H), 7.19 (dd, $^3J$ = 4.3 Hz, $^4J$ = 2.0 Hz, 1H),7.03 (b, 1H), 6.74 (b, 1H), 2.54 (s, 3H), 2.533 (s, 3H),2.529 (s, 3H), 2.48 (s, 3H), 0.89 (dq, $^2J$ = 9.3 Hz, $^3J$ = 7.0 Hz, 2H), 0.86 (dq, $^2J$ = 9.3 Hz, $^3J$ = 7.0 Hz, 2H), −0.82 (t, $^3J$ = 7.0 Hz, 6H); $^{13}$C NMR (150 MHz, $CDCl_3$, 300 K) $\delta_C$ = 180.8, 172.4, 164.1, 154.1, 151.2, 142.0, 138.6, 138.3, 137.9, 137.7, 137.6, 137.3, 137.0, 136.6, 136.4, 135.7, 135.0, 134.5, 133.7, 133.1, 133.0, 131.4, 131.2, 131.1, 130.9, 128.5, 128.1, 128.0, 127.7, 124.0, 122.7, 121.5, 116.7, 108.3, 98.1, 58.2, 21.6, 21.41, 21.38, 21.36, 13.0; UV−vis ($CH_2Cl_2$, 298 K) $\lambda$/nm ($\varepsilon$/$M^{-1}$ $cm^{-1}$) = 319 (31600), 358 (27200), 400 (sh), 426 (sh) 450 (105000), 531 (2700), 575 (4500), 626 (sh), 688 (14000), 735 (19000); HRMS (ESI-TOF) $m/z$ = 775.3634 (obsd), 775.3643 (calcd for $C_{52}H_{47}N_4O_3$, $[M + H]^+$).

**Reaction of 1-$Me_3$ with Brine.** A solution of **1**-$Me_3$ (2 mg) in dichloromethane (5 mL) was stirred vigorously for 2 h with saturated aqueous NaCl (5 mL). The organic layer was then washed with five portions of water (10 mL each), and the solvent was evaporated in vacuum. The conversion and yields were examined by integration of the $^1$H NMR signals ($CDCl_3$) revealing the presence of 36% of **4**-$Me_2$, 19% of **3**-$Me_2$, and 45% of starting **3**-$Me_3$.

**Crystallographic Data.** The structures were solved by direct methods using the SHELXS program.[69] All non-hydrogen atoms were refined anisotropically by full matrix least-squares with SHELXL-97.[69] All H atoms were placed in a calculated position and refined as the riding model with $U_{iso}$(H) = 1.2$U_{eq}$(C).

X-ray quality crystals of **1**-$Et_3$ were obtained by slow diffusion of an ethyl acetate solution of **3**-$Et_3$ into hexane at room temperature. Crystal data for **1**-$Et_3$: $C_{55}H_{51}N_5O_3$, $M_r$ = 830.01, $T$ = 100(2) K, Cu K$\alpha$ radiation, triclinic, space group $P\bar{1}$, $a$ = 14.124(7) Å, $b$ = 14.642 (6) Å, $c$ = 16.533(9) Å, $\alpha$ = 113.02(4)°, $\beta$ = 96.96(4)°, $\gamma$ = 113.94 (5)°, $V$ = 2712.1(2) Å$^3$, $Z$ = 2, $D_c$ = 1.016 Mg $m^{-3}$, $\lambda$ = 1.54178 Å, $\mu$ = 0.498 $mm^{-1}$, diffractometer with CCD detector, 3.08° ≤ $\theta$ ≤ 66.00°, 17283 collected reflections, 9264 independent reflections, 606 parameters, $R_1(F)$ = 0.083, $wR_2(F^2)$ = 0.2254, $S$ = 1.385, largest difference peak and hole 0.781 and −0.464 e·Å$^{-3}$. The external oxygen atom is disordered, which we modeled by displacing its electron density into two sites, O3 and O3A. The less occupied site (18%) is located 1.24(1) Å from the N2 site.

X-ray quality crystals of **2** were obtained by slow diffusion of a chloroform solution of **2** into hexane at room temperature. Crystal data for **2**: $C_{50}H_{41}N_4O$, $M_r$ = 749.32, $T$ = 100(2) K, Mo K$\alpha$ radiation, triclinic, space group $P\bar{1}$, $a$ = 9.463(1) Å, $b$ = 14.978(1) Å, $c$ = 15.103(2) Å, $\alpha$ = 69.75(9)°, $\beta$ = 80.70(9)°, $\gamma$ = 73.91(9)°, $V$ = 1924.7(3) Å$^3$, $Z$ = 2, $D_c$ = 1.293 Mg $m^{-3}$, $\lambda$ = 0.71073 Å, $\mu$ = 0.144 $mm^{-1}$, diffractometer with CCD detector, 2.79° ≤ $\theta$ ≤ 26.50°, 7868 collected reflections, 1467 independent reflections, 505 parameters, $R_1(F)$ = 0.066, $wR_2(F^2)$ = 0.0839, $S$ = 0.635, largest difference peak and hole 0.430 and −0.341 e·Å$^{-3}$.

X-ray quality crystals of **4**-$Me_2$ were obtained by slow diffusion of a chloroform solution of **4**-$Me_2$ into hexane at room temperature. Crystal data for **4**-$Me_2$: $C_{52}H_{44}Cl_3N_4O_3$, $M_r$ = 985.61, $T$ = 100(2) K, Mo K$\alpha$ radiation, monoclinic, space group $P2_1/c$, $a$ = 12.550(7) Å, $b$ = 29.401(1) Å, $c$ = 12.857(7) Å, $\alpha$ = 90.00°, $\beta$ = 92.94(5)°, $\gamma$ = 90.00°, $V$ = 4737.6(4) Å$^3$, $Z$ = 4, $D_c$ = 1.382 Mg $m^{-3}$, $\lambda$ = 0.71073 Å, $\mu$ = 0.411 $mm^{-1}$, diffractometer with CCD detector, 3.04° ≤ $\theta$ ≤ 27.00°, 10330 collected reflections, 3795 independent reflections, 628 parameters, $R_1(F)$ = 0.059, $wR_2(F^2)$ = 0.1648, $S$ = 0.734, largest difference peak and hole 0.442 and −0.436 e·Å$^{-3}$. The asymmetric unit contains one molecule of **4**-$Me_2$ and two molecules of chloroform solvent, and one of them is disordered into two sites. The external oxygen of **4**-$Me_2$ atom is disordered, which we modeled by displacing its electron density into two sites, O3 and O3A. The less occupied site (29%) is located 1.208(8) Å from the N2 site.

X-ray quality crystals of **3**-EtMe were obtained by slow diffusion of a chloroform solution of **3**-EtMe into methanol at room temperature. Crystal data for **3**-EtMe: $C_{51}H_{44}N_4O_2$, $M_r$ = 744.90, $T$ = 100(2) K, Mo K$\alpha$ radiation, monoclinic, space group $P2_1/n$, $a$ = 11.5264(2) Å, $b$ = 26.2557(4) Å, $c$ = 13.4965(2) Å, $\alpha$ = 90.00°, $\beta$ = 91.037 (1) °, $\gamma$ = 90.00°, $V$ = 4083.8 (1) $^3$, $Z$ = 4, $D_c$ = 1.212 Mg $m^{-3}$, $\lambda$ = 0.71073 Å, $\mu$ = 0.074 $mm^{-1}$, diffractometer with CCD detector, 2.92° ≤ $\theta$ ≤ 27.00°, 49655 collected reflections, 8913 independent reflections, 524 parameters, $R_1(F)$ = 0.058, $wR_2(F^2)$ = 0.2225, $S$ = 0.925, largest difference peak and hole 0.698 and −0.468 e·Å$^{-3}$. The external oxygen atom is disordered, which we modeled by displacing its electron density into two sites, O2 and O2A. The less occupied site (17%) is located 1.317(7) Å from the N2 site.

The crystal structures have been deposited at the Cambridge Crystallographic Data Center and allocated the deposition numbers CCDC 896020−896023.

## ■ ASSOCIATED CONTENT

### Ⓢ Supporting Information

Crystallographic data in cif format, selected bond lengths and hydrogen bond geometries in the crystal structures (Tables S1 and S2), 1D and 2D NMR, and mass spectra. This material is available free of charge via the Internet at http://pubs.acs.org.

## ■ AUTHOR INFORMATION

### Corresponding Author

*E-mail: lixiaofang@iccas.ac.cn; piotr.chmielewski@chem.uni.wroc.pl.

### Notes

The authors declare no competing financial interest.

## ■ ACKNOWLEDGMENTS

This work was supported by National Natural Science Foundation of China (No. 20971041), the Key Project of Chinese Ministry of Education (No. 210146).

## ■ REFERENCES

(1) Chmielewski, P. J.; Latos-Grażyński, L.; Rachlewicz, K.; Głowiak, T. *Angew. Chem., Int. Ed. Engl.* **1994**, *33*, 779−781.
(2) Furuta, H.; Asano, T.; Ogawa, T. *J. Am. Chem. Soc.* **1994**, *116*, 767−768.
(3) Geier, G. R., III; Haynes, D. M.; Lindsey, J. S. *Org. Lett.* **1999**, *1*, 1455−1458.
(4) Liu, B. Y.; Brückner, C.; Dolphin, D. *Chem. Commun.* **1996**, 2141−2142.
(5) Lash, T. D.; Richter, D. T.; Shiner, C. M. *J. Org. Chem.* **1999**, *64*, 7973−7982.
(6) Li, X.; Liu, B.; Yu, X.; Yi, P.; Yi, R.; Chmielewski, P. J. *J. Org. Chem.* **2012**, *77*, 2431−2440.
(7) Chmielewski, P. J.; Latos-Grażyński, L. *J. Chem. Soc., Perkin Trans. 2* **1995**, 503−509.
(8) Chmielewski, P. J. *Org. Lett.* **2005**, *7*, 1789−1792.
(9) Chmielewski, P. J. *Inorg. Chem.* **2009**, *48*, 432−445.
(10) Qu, W.; Ding, T.; Cetin, A.; Harvey, J. D.; Taschner, M. J.; Ziegler, C. J. *J. Org. Chem.* **2006**, *71*, 811−814.
(11) Schmidt, I.; Chmielewski, P. J. *Tetrahedron Lett.* **2001**, *42*, 1151−1154.
(12) Schmidt, I.; Chmielewski, P. J. *Tetrahedron Lett.* **2001**, *42*, 6389−6392.
(13) Chmielewski, P. J.; Maciołek, J.; Szterenberg, L. *Eur. J. Org. Chem.* **2009**, 3930−3939.
(14) Li, X.; Liu, B.; Yi, P.; Yi, R.; Yu, X.; Chmielewski, P. J. *J. Org. Chem.* **2011**, *76*, 2345−2349.
(15) Chmielewski, P. J. *Angew. Chem., Int. Ed.* **2004**, *43*, 5655−5658.
(16) Furuta, H.; Ishizuka, T.; Osuka, A.; Ogawa, T. *J. Am. Chem. Soc.* **1999**, *121*, 2945−2946.
(17) Toganoh, M.; Kimura, T.; Furuta, H. *Chem.—Eur. J.* **2008**, *14*, 10585−10594.
(18) Toganoh, M.; Kimura, T.; Furuta, H. *Chem. Commun.* **2008**, 102−104.
(19) Ishikawa, Y.; Yoshida, I.; Akaiwa, K.; Koguchi, E.; Sasaki, T.; Furuta, H. *Chem. Lett.* **1997**, 453−454.
(20) Ching, W.-M.; Hung, C.-H. *Chem. Commun.* **2012**, *48*, 4989−4991.
(21) Chmielewski, P. J.; Latos-Grażyński, L.; Głowiak, T. *J. Am. Chem. Soc.* **1996**, *118*, 5690−5701.
(22) Chmielewski, P. J.; Latos-Grażyński, L. *Inorg. Chem.* **2000**, *39*, 5639−5647.
(23) Schmidt, I.; Chmielewski, P. J. *Chem. Commun.* **2002**, 92−93.
(24) Schmidt, I.; Chmielewski, P. J.; Ciunik, Z. *J. Org. Chem.* **2002**, *67*, 8917−8927.
(25) Schmidt, I.; Chmielewski, P. J. *Inorg. Chem.* **2003**, *42*, 5579−5593.
(26) Chmielewski, P. J. *Inorg. Chem.* **2007**, *46*, 1617−1626.
(27) Ishizuka, T.; Osuka, A.; Furuta, H. *Angew. Chem., Int. Ed.* **2004**, *43*, 5077−5081.
(28) Rachlewicz, K.; Wang, S.-L.; Ko, J.-L.; Hung, C.-H.; Latos-Grażyński, L. *J. Am. Chem. Soc.* **2004**, *126*, 4420−4431.
(29) Hung, C.-H.; Wang, S.-L.; Ko, J.-L.; Peng, C.-H.; Hu, C.-H.; Lee, M.-T. *Org. Lett.* **2004**, *6*, 1393−1396.
(30) Grzegorzek, N.; Pawlicki, M.; Latos-Grażyński, L. *J. Org. Chem.* **2009**, *74*, 8547−8553.
(31) Chmielewski, P. J.; Szterenberg, L.; Siczek, M. *Chem.—Eur. J.* **2011**, *17*, 1009−1020.
(32) Ishizuka, T.; Ikeda, S.; Toganoh, M.; Yoshida, I.; Ishikawa, Y.; Osuka, A.; Furuta, H. *Tetrahedron* **2008**, *64*, 4037−4050.
(33) Młodzianowska, A.; Latos-Grażyński, L.; Szterenberg, L.; Stępień, M. *Inorg. Chem.* **2007**, *46*, 6950−6957.
(34) Młodzianowska, A.; Latos-Grażyński, L.; Szterenberg, L. *Inorg. Chem.* **2008**, *47*, 6364−6374.
(35) Xiao, Z.; Patrick, B. O.; Dolphin, D. *Chem. Commun.* **2002**, 1816−1817.
(36) Li, X.; Chmielewski, P. J.; Xiang, J.; Xu, J.; Li, Y.; Liu, H.; Zhu, D. *Org. Lett.* **2006**, *8*, 1137−1140.
(37) Li, X.; Chmielewski, P. J.; Xiang, J.; Xu, J.; Jiang, L.; Li, Y.; Liu, H.; Zhu, D. *J. Org. Chem.* **2006**, *71*, 9739−9742.
(38) Chmielewski, P. J.; Schmidt, I. *Inorg. Chem.* **2004**, *43*, 1885−1894.
(39) Harvey, J. D.; Ziegler, C. J. *Coord. Chem. Rev.* **2003**, *247*, 1−19.
(40) Chmielewski, P. J.; Latos-Grażyński, L. *Coord. Chem. Rev.* **2005**, *249*, 2510−2533.
(41) Chmielewski, P. J. *Angew. Chem., Int. Ed.* **2005**, *44*, 6417−6420.
(42) Siczek, M.; Chmielewski, P. J. *Angew. Chem., Int. Ed.* **2007**, *46*, 7432−7436.
(43) Chmielewski, P. J.; Durlej, B.; Siczek, M.; Szterenberg, L. *Angew. Chem., Int. Ed.* **2009**, *48*, 8736−8739.
(44) Toganoh, M.; Miyachi, T.; Akimaru, H.; Ito, F.; Nagamura, T.; Furuta, H. *Org. Biomol. Chem.* **2009**, *7*, 3027−3030.
(45) Chmielewski, P. J.; Siczek, M.; Szterenberg, L. *Inorg. Chem.* **2011**, *50*, 6719−6736.
(46) Maeda, H.; Morimoto, T.; Osuka, A.; Furuta, H. *Chem.—Asian J.* **2006**, *1*, 832−844.
(47) Furuta, H.; Nanami, H.; Morimoto, T.; Ogawa, T.; Kral, V.; Sessler, J. L.; Lynch, V. *Chem.—Asian J.* **2008**, *3*, 592−599.
(48) Jiang, H.-W.; Hao, F.; Chen, Q.-Y.; Xiao, J.-C.; Liu, S. B.; Gu, Y.-C. *J. Org. Chem.* **2010**, *75*, 3511−3514.
(49) Hayes, M. J.; Spence, J. D.; Lash, T. D. *Chem. Commun.* **1998**, 2409−2410.
(50) Lash, T. D.; Muckey, M. A.; Hayes, M. J.; Liu, D.; Spence, J. D.; Ferrence, G. M. *J. Org. Chem.* **2003**, *68*, 8558−8570.
(51) Hung, C.-H.; Chen, W.-C.; Lee, G.-H.; Peng, S.-M. *Chem. Commun.* **2002**, 1516−1517.
(52) Grampp, G.; Landgraf, S.; Rasmussen, K. *J. Chem. Soc., Perkin Trans. 2* **1999**, 1897−1899.
(53) Rasmussen, K.; Hussain, T.; Landgraf, S.; Grampp, G. *J. Phys. Chem. A* **2012**, *116*, 193−198.
(54) Xiao, Z.; Patrick, B. O.; Dolphin, D. *Chem. Commun.* **2003**, 1062−1063.
(55) Stępień, M.; Latos-Grażyński, L.; Lash, T. D.; Szterenberg, L. *Inorg. Chem.* **2001**, *40*, 6892−6900.
(56) Furuta, H.; Ishizuka, T.; Osuka, A.; Dejima, H.; Nakagawa, H.; Ishikawa, Y. *J. Am. Chem. Soc.* **2001**, *123*, 6207−6208.
(57) Chmielewski, P. J.; Maciołek, J. *Chem. Commun.* **2012**, *48*, 428−430.
(58) Pratt, E. F.; Draper, J. D. *J. Am. Chem. Soc.* **1949**, *71*, 2846−2849.
(59) Stępień, M.; Sessler, J. L. *Org. Lett.* **2007**, *9*, 4785−4787.
(60) Kihara, N.; Kidoba, K. *Org. Lett.* **2009**, *11*, 1313−1316.
(61) Shah, S. T. A.; Singh, S.; Guiry, P. J. *J. Org. Chem.* **2009**, *74*, 2179−2182.
(62) Caras-Quintero, D.; Bäuerle, P. *Chem. Commun.* **2004**, 926−927.
(63) Zoltewicz, J. A.; Sale, A. A. *J. Org. Chem.* **1970**, *35*, 3462−3467.
(64) Novakova, V.; Miletin, M.; Kopecky, K.; Franzová, Š.; Zimcik, P. *Eur. J. Org. Chem.* **2011**, 5879−5886.
(65) Bai, Z.; Gao, Y.; Zhu, P.; Bian, Y.; Jiang, J. *Inorg. Chem.* **2010**, *49*, 9005−9011.
(66) Lehn, J.-M. *Prog. Polym. Sci.* **2005**, *30*, 814−831.
(67) Mayer, C. D.; Joiner, C. S.; Stoddart, J. F. *Chem. Soc. Rev.* **2007**, *36*, 1705−1723.
(68) Rowan, S. J.; Cantrill, S. J.; Cousins, G. R. L.; Sanders, J. K. M.; Stoddart, J. F. *Angew. Chem., Int. Ed.* **2002**, *41*, 898−952.
(69) Sheldrick, G. M. *Acta Crystallogr.* **2008**, *A64*, 112−122.